Experimental and Computational Study of the Association between Vitamin B_{12} and Glutathione in type 2 Diabetes

Masters Thesis

Varun Karamshetty

April 2, 2014

Supervisor:
Dr. Pranay Goel

Dept. of Mathematics
Indian Institute of Science Education and Research, Pune

Certificate

This is to certify that this thesis entitled **Experimental and Computational Study of the Association between Vitamin B_{12} and Glutathione in type 2 Diabetes** submitted towards the partial fulfilment of the BS-MS dual degree programme at the Indian Institute of Science Education and Research Pune represents original research carried out by **Varun Karamshetty** at **Indian Institute of Science Education and Research, Pune**, under the supervision of **Dr. Pranay Goel**, Dept. of Mathematics and Biology, IISER Pune during the academic year 2013-2014.

Thesis Advisory Committee
Dr. Pranay Goel
Dr. Saroj Ghaskadbi

Prof. A. Raghuram
Coordinator of Maths Faculty

Dedicated to Amma and Papa

Abstract

Diabetes mellitus is a growing problem in large parts of India, where the population is vegetarian, and vitamin B_{12} deficient. We ask if prevalent vitamin B_{12} deficiency is related to the rising number of diabetic patients. We tested newly diagnosed Indian diabetic patients for correlation between their vitamin B_{12} and GSH, and found it to be weak. We then examined the theoretical dependence of GSH on vitamin B_{12} with a mathematical model of 1-carbon metabolism due to Reed and co-workers. We found that the lack of correlation is due to homeostasis of homocysteine despite large variation in the activity of methionine synthase, a co-enzyme of vitamin B_{12}. We therefore studied the methionine cycle in the Reed-Nijhout model in greater detail: We first constructed a reduced methionine cycle model extracted from the full network, and then based on that we developed a simple analytically tractable 'stylized model' that captures the essential topology. We find – counter-intuitively – that the flux responsible for homeostasis of homocysteine is actually peripheral to the methionine cycle. These results suggest (i) a natural explanation of why GSH is observed to be independent of vitamin B_{12}, despite being downstream of it in the metabolic network, and (ii) that the clinically observed symptom of vitamin B_{12} deficiency, hyperhomocysteinemia, is not due to a simple "remethylation-block", as is commonly argued.

Contents

Chapter 1

Introduction

Diabetes mellitus is a group of metabolic diseases in which the patient has high blood sugar levels. The high blood sugar is caused due to a lack of – or a perceived lack of – insulin, which is responsible for keeping blood sugar at a healthy level. Type 1 diabetes is caused due to insufficient production of insulin by the pancreas. Type 2 diabetes is caused when the cells in the body do not respond to the insulin produced. β-cells are a type of cells in the pancreas that are primarily responsible for storing and releasing insulin.

Saroj Ghaskadbi and Pranay Goel et al. have been working on the effects of oxidative stress in Diabetic patients (private communication with Dr. Goel). There exist several reports that demonstrate increased oxidative stress in diabetic patients. Acharya et al. [1] measured the oxidative stress parameters (OSP) in diabetic patients, serially from the time of diagnosis, and showed that improved OSP related to an improved β-cell function.

Glutathione (GSH) is an important anti-oxidant species, both in the blood and cytosol. Goel et al., have showed that GSH levels are usually below 450 μM in diabetic patients (private communication with Dr. Goel). The GSH synthesis mechanism is showed in the Reed-Nijhout model of 1-carbon and glutathione metabolism (taken without permission from [2]) in the appendix to this document. The 1-carbon metabolism and glutathione synthesis mechanism is critical for nucleotide synthesis, oxidant defense, and the synthesis of Hcy.

Vitamin B_{12}, one of the eight B vitamins, plays a key role in the synthesis of glutathione. Vitamin B_{12} is a co-enzyme to the Methionine Synthase (MS), which catalyzes the remethylation of homocysteine (Hcy) into methionine (Met), in the methionine cycle. The methionine cycle is a part of the 1-carbon metabolism and glutathione synthesis mechanism.

In large parts of India – where diabetes is developing rapidly – the population is vegetarian, and suffers from a vitamin B_{12} deficiency. Antony [3], Stabler and Allen [4] have argued that vegetarianism is a possible reason for prevalent vitamin B_{12} deficiency among Indians, although Refsum et al. [5] show that vegetarian diet only partly explains the high prevalence of cobalamin deficiency in India. Yajnik et al. [6], in their Pune Maternal Nutrition study, show that the offspring of the mothers with a combination of high folate and low vitamin B_{12} concentrations were the most insulin resistant. In this thesis we try to answer if there is any potential causal link between vegetarianism, the prevalence of vitamin B_{12} deficiency among Indians and the growing incidence of diabetes.

Chapter 2

Analysis of GSH, Folate and Vitamin B_{12} Data

This data was collected by Jhankar Acharya and Saroj Ghaskadbi as a part of the clinical study described in [1]. Newly diagnosed diabetic patients were followed over the first 8 weeks of their anti-diabetic therapy. A wide variety of blood parameters were collected including GSH and other oxidative stress bio-markers. Data was collected at the beginning of treatment, and at 4 and 8 weeks subsequently.

Fig. 2.1 shows GSH levels plotted against vitamin B_{12} concentrations for 182 individuals. The individuals were classified into four groups based on their vitamin B_{12} deficiency status and diabetic/non-diabetic status. Glutathione concentration of 450 μM was taken to be the cut-off for oxidative stress levels. Individuals below this level are usually diabetic. Vitamin B_{12} concentration of 148 pM was considered to be the cut-off under which the individuals were considered to be vitamin B_{12} deficient[7].

We used the Curve Fitting Toolbox of MATLAB® for performing the regression analysis and plotting the figures shown below. We have used simple linear regression techniques to fit the data points to the regression equations described below.

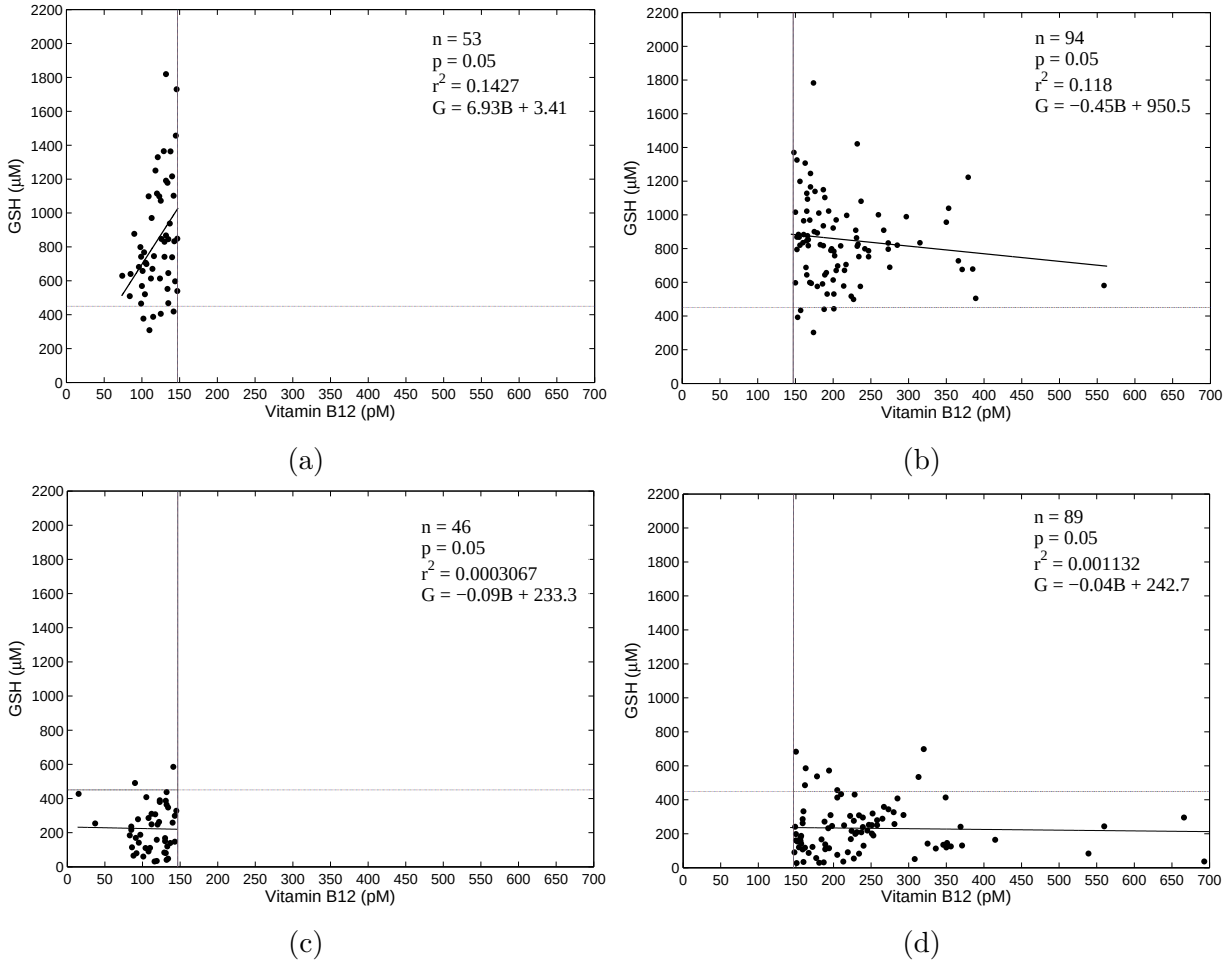

Figure 2.1: **GSH and vitamin B_{12} are weakly correlated in diabetes.** Linear regression between blood GSH and vitamin B_{12} for non-diabetic control subjects **(a, b)** and diabetic patients **(c, d):**. Individuals with serum vitamin B_{12} <148 pM are considered vitamin B_{12} deficient [7]. Thus panels **(a, c)** represent vitamin B_{12} deficiency. A GSH value of 450 μM is taken as a cut-off of oxidative stress. In the regression equations, **G** stands for Glutathione levels in μM and **B** stands for vitamin B_{12} concentration in pM.

As can be observed in Fig. 2.1, GSH levels in both diabetics and control subjects is uncorrelated with vitamin B_{12} concentration. There is no strong correlation between GSH levels and vitamin B_{12} concentrations in each of the four categories of patients considered. This is very intriguing because vitamin B_{12} acts in our body through Methionine Synthase, whose activity is directly upstream of GSH synthesis.

Fig. 2.2 shows GSH levels plotted against folate concentrations for diabetics (blue and green; n=135) and controls (red and cyan; n=147). Glutathione concentration of 450 μM is taken to be the cut-off below which the individuals are usually diabetic. Folate concentration of 7nM was considered to be the cut-off below which the individuals were considered folate deficient (diabetic and folate deficient - Blue, n=11; Control and Folate deficient - Red, n=5) [8].

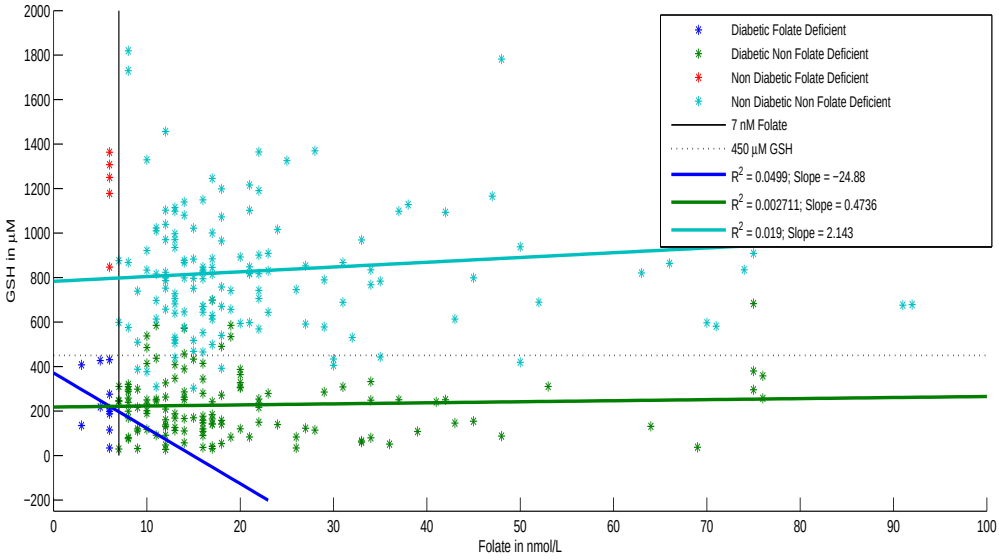

Figure 2.2: Scatter plot GSH level vs Folate concentration

As can be observed in Fig. 2.2 the GSH level in both diabetics and control patients is uncorrelated with folate concentration. There is no strong correlation between GSH levels and folate concentrations in all the four categories of patients considered: Diabetic patients with folate deficiency (Blue), Diabetic patients with no folate deficiency (Green), Non-diabetic patients with folate deficiency (Red) or Non-diabetic patients with no folate deficiency (Cyan).

To understand the reasons underlying the lack of correlation between GSH and vitamin B_{12} levels, as shown in Fig. 2.1, we look at a mathematical model of 1-Carbon Glutathione metabolism, originally due to Reed et al [2].

Chapter 3

Vitamin B_{12} deficiency in the computational model

We are using a computational model of 1-carbon metabolism and glutathione synthesis due to Reed et al. [2, 9, 10, 8, 11]. The .ode (Office Object Data Embedding) file we used was taken from the European Bioinformatics Institute's models database and was encoded by Lukas Endler. It is available, for download, at `http://www.ebi.ac.uk`. We will henceforth refer to this model as the "Reed-Nijhout model".

3.1 Validating the model

The model encoded by Endler contains a feeding rhythm; parameters named *breakfast*, *lunch*, *dinner* and *fasting* were used to describe the relative level of Amino Acids in the blood by using a time-step function named *aa_input*. We removed the daily feeding rhythm when using this model for our computations.

To validate the model downloaded, we reproduce some figures from Reed et al.'s [2]'s work using Endler's model. The figures used in the comparisons below are extracted from Reed et al.'s work [2] without their permission. What follows is a comparison of the figures generated using Endler's model and Reed et al.'s [2] originals.

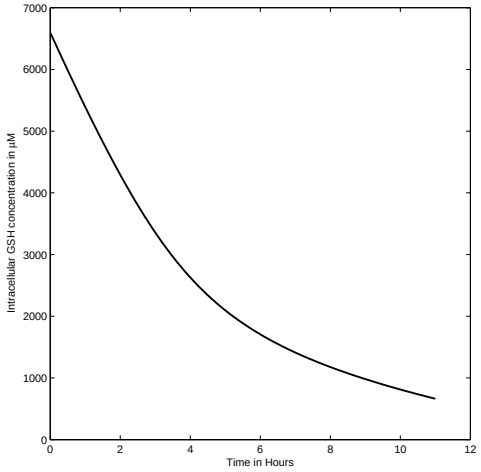

(a)

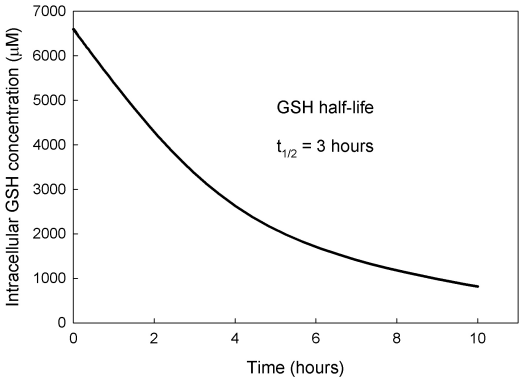

(b)

Figure 3.1: **Intracellular GSH concentration in the model when GSH synthesis is completely inhibited**. The panel on the right shows the original Fig. taken without permission from Reed et al. [2]'s work (Fig. 2 in [2]), whereas the panel on the left is our reproduction. GSH synthesis is completely inhibited in the Reed-Nijhout model by setting the concentration of the enzyme GCS to zero. It can be seen that both the figures agree very well.

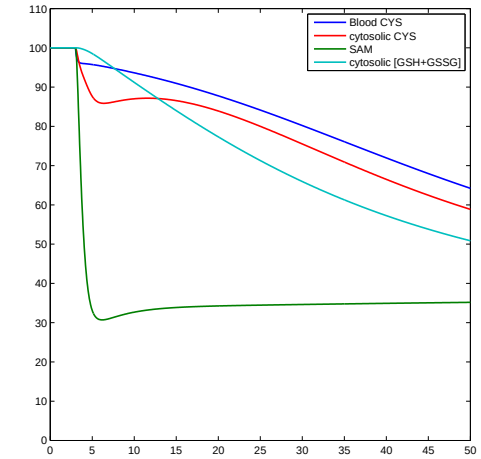

(a)

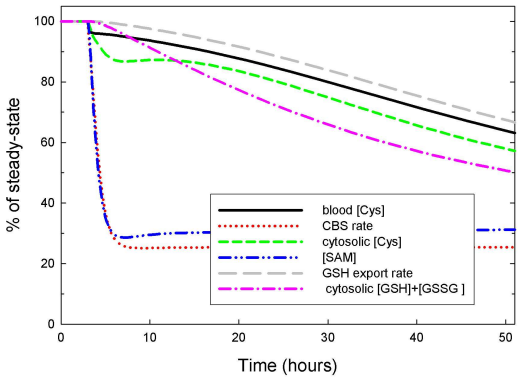

(b)

Figure 3.2: **Concentration of GSH and other metabolites during fasting.** The panel on the right shows the original Fig. taken without permission from Reed et al. [2]'s work (Fig. 3 in [2]), whereas the panel on the left is our reproduction. The conditions of fasting are simulated in the model by reducing the inputs of cysteine, methionine, glycine, glutamate, and serine to 1/3 of normal after the first three hours. It can be seen that the components in both the panels show similar plots.

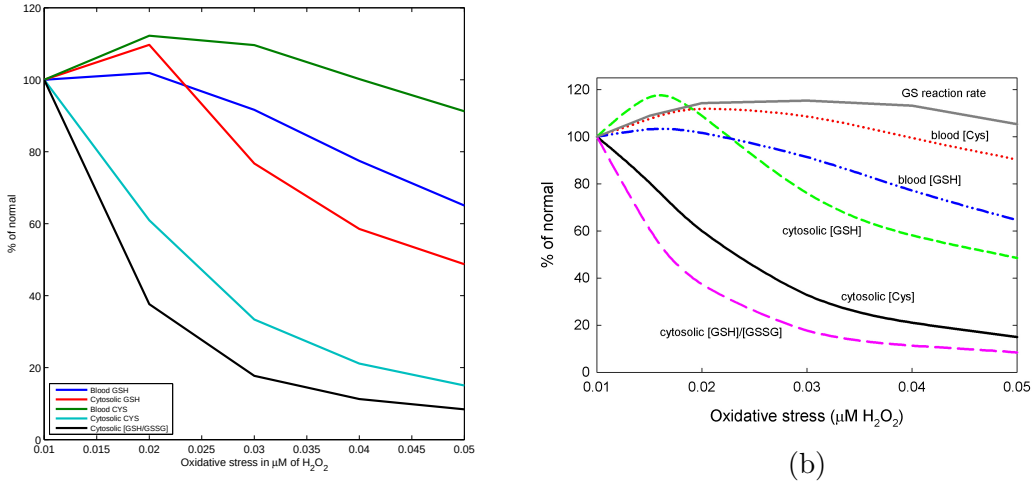

Figure 3.3: **Effect of oxidative stress.** The panel on the right shows the original Fig. taken without permission from Reed et al. [2]'s work (Fig. 6 in [2]), whereas the panel on the left is our reproduction. Oxidative stress is varied in the Reed-Nijhout model by changing the value of the parameter "H_2O_2" in the model. It can be seen that both the plots are identical.

Figs. 3.1, 3.2 and 3.3 show that the computational model encoded by Lukas Endler (referred to as "Reed-Nijhout" model henceforth) is in agreement with the model proposed by Reed et al. Hence, we use this model to observe the effect of vitamin B_{12} deficiency on Glutathione synthesis.

3.2 Simulating Vitamin B_{12} Deficiency

Vitamin B_{12} participates in glutathione synthesis by acting as a co-enzyme for 5-methyltetrahydrofolate-homocysteine methyltransferase, also known as methionine synthase (MS). MS catalyzes the remethylation of methionine (Met) from homocysteine (Hcy) in the methionine cycle (refer Appendix). Vitamin B_{12} also acts a co-factor in the conversion of methylmalonyl-CoA into succinyl-CoA by methylmalonlyl-CoA mutase.

In the Reed-Nijhout model, a vitamin B_{12} deficient scenario is simulated by inhibiting the activity of MS. MS activity is regulated by the parameter V_{max}^{MS} whose standard value is 500 μM/hr. Setting V_{max}^{MS} to a value lesser than 500 μM/hr is equivalent to establishing a vitamin B_{12} deficient scenario in the Reed-Nijhout model. Reed and Nijhout et al. have used this technique to establish vitamin B_{12} deficiency in the model, in their earlier work [8].

V_{max}^{MS} was varied over three orders of magnitude ranging from 5 to 5,000, in the Reed-Nijhout model and the effects were observed. Fig. 3.4 shows the changes in glutathione with V_{max}^{MS}.

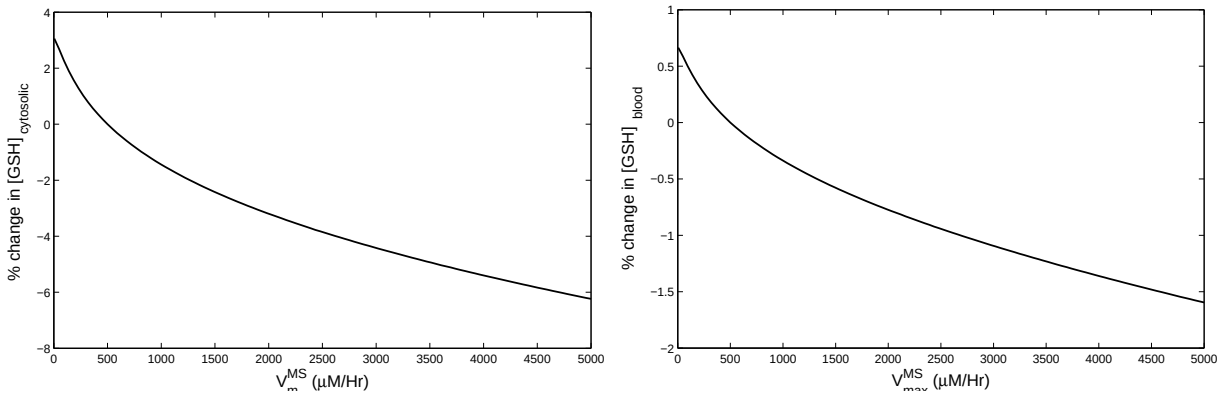

(a) (b)

Figure 3.4: **Glutathione steady state vs V_{max}^{MS}.** The panel on the left shows the steady state concentrations of cytosolic glutathione with respect to V_{max}^{MS}, whereas the panel on the right shows the blood glutathione levels. Glutathione levels, both in blood and cytosol, vary by insignificant amounts despite V_{max}^{MS} changing over three orders of magnitude. This shows that glutathione levels are insensitive to changes in V_{max}^{MS}.

From Fig. 3.4, it can be observed that the maximum change in the glutathione (GSH) levels is only about 4% despite V_{max}^{MS} being varied by three orders of dimension. This is in line with our observations, in Fig. 2.1, where GSH was found to be uncorrelated with vitamin B_{12} levels. This lack of effect on GSH is surprising because vitamin B_{12} activity is directly upstream of GSH (refer Fig. in the appendix).

To understand this lack of sensitivity better, we systematically look at all the metabolites upstream of GSH leading up to the MS activity in the methionine cycle. Fig. 3.5 below shows the percentage changes in various metabolites, upstream of GSH, as V_{max}^{MS} is changed.

3.3 Hcy exhibits homeostasis in the Reed-Nijhout model

We systematically observed all the metabolites upstream of GSH in order to track down the exact node where the lack of sensitivity originates. We plot graphs showing the variation of Cyt, Cys, Hcy, Met, SAM and SAH with changes in V_{max}^{MS}. As has been described earlier Hcy, Met, SAM and SAH form the methionine cycle.

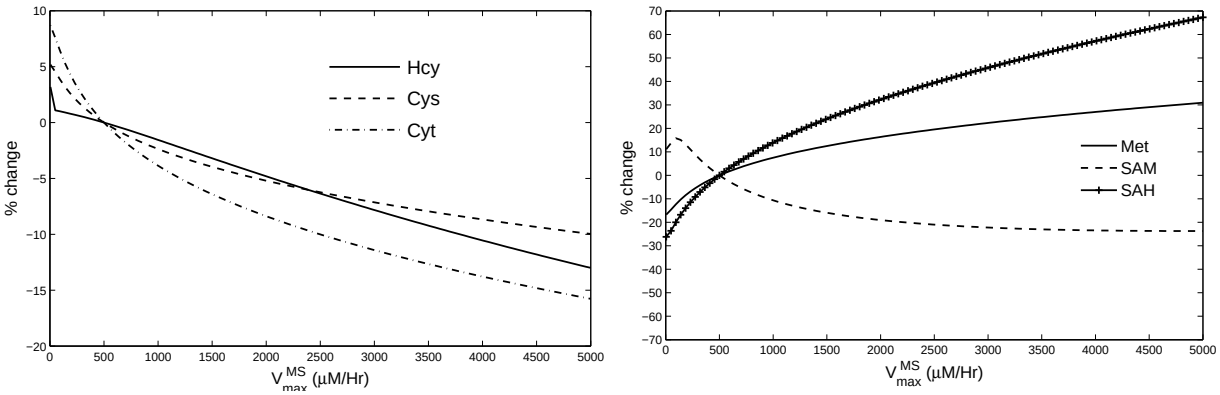

(a) (b)

Figure 3.5: **Hcy buffers changes in vitamin B_{12}.** Percentage variation in the steady state values of **(a):** species upstream of GSH leading up to Hcy, *viz.*, cysteine (Cys), cystathionine (Cyt); **(b):** species upstream of Hcy, *viz.*, Met, SAM and SAH. The variations are calculated with respect to steady state value of each specie at $V_{max}^{MS} = 500$ in the Reed-Nijhout model. It can be observed that the species shown in the figure on the right-hand side vary significantly whereas the species on the left-hand side vary by only about 15% displaying buffering against changes in V_{max}^{MS} .

It can be seen from Fig. 3.5, that Met, SAM and SAH vary significantly with V_{max}^{MS} whereas the variation in Hcy is not as pronounced. The effect of the changes in V_{max}^{MS} is lost at Hcy and does not percolate systematically to metabolites downstream of it. This implies that Hcy, and the metabolites downstream of it, are insensitive to changes in vitamin B_{12} levels.

This is quite intriguing because it is clinically accepted that vitamin B_{12} deficiency leads to hyperhomocysteinemia – an abnormally high level of homocysteine. Our computational model, by predicting that Hcy remains unaffected in face of V_{max}^{MS} variation, directly contradicts this clinically accepted theory. We try to explain the reasons behind this prediction by observing the methionine cycle more carefully.

Chapter 4

Reduced Model

To understand the reasons leading to homeostasis of Hcy despite huge variations in V_{max}^{MS} we focus our attention on a small sub-network of the Reed-Nijhout model: methionine cycle.

The gist of the methionine cycle is shown in Fig. 4.1. In the methionine cycle, Met is converted to SAM, SAM is converted to SAH, SAH is converted to Hcy and Hcy is re-methylated to form Met. Various enzymes, like GNMT, BHMT, SAHH and MAT1, catalyze different legs of this cycle. The remethylation of Hcy to Met is catalyzed by MS, with vitamin B_{12} acting as a co-enzyme for this conversion.

We try to gain a better understanding of the mass-action equations governing the metabolites in the methionine cycle, in order to explain the Hcy homeostasis. We do this by building a methionine cycle motif extracted from the full Reed-Nijhout model. The construction of this methionine cycle motif is explained in the following section.

4.1 Constructing the Reduced Model

In order to understand the Hcy homeostasis, we study the methionine cycle in greater detail. We start by carefully extracting the methionine cycle sub-network from the Reed-Nijhout model and accounting for the fluxes moving in and out of this sub-network, connecting it with the Reed-Nijhout model.

Fig. 4.1 shows the methionine cycle and the enzymes catalyzing different parts of the cycle.

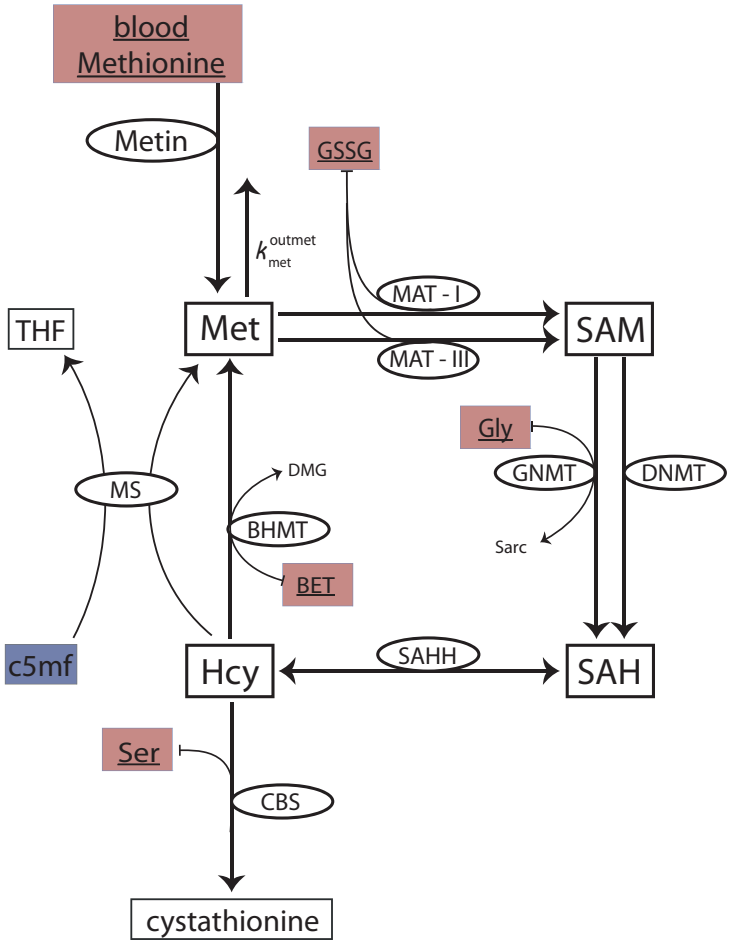

Figure 4.1: **The methionine cycle.** The diagram shows the metabolites constituting the methionine cycle, *viz.*, Hcy, Met, SAM and SAH, along with the enzymes catalyzing the inter-conversions. The enzymes are depicted in ellipses. c5mf, which we have fit using a phenomenological function is depicted in a box with a blue tint. Other metabolites which were approximated as constants in the reduced model are shown in boxes with a maroon tint.

The mass action equations for the metabolites constituting the methionine cycle are written as follows in the full Reed-Nijhout model:

$$\textbf{hcy'} = J_{SAHH} - J_{MS} - J_{BHMT} - J_{CBS} \tag{4.1}$$
$$\textbf{met'} = J_{bMETc} + J_{MS} + J_{BHMT} - J_{MAT1} - J_{MAT3} \tag{4.2}$$
$$\textbf{sam'} = J_{MAT1} + J_{MAT3} - J_{GNMT} - J_{DNMT} \tag{4.3}$$
$$\textbf{sah'} = J_{GNMT} - J_{DNMT} - J_{SAHH} \tag{4.4}$$

In the above equations, J_{MS} stands for the reaction velocity corresponding to the enzyme MS. Each of the above reaction velocities are defined by the following expressions:

$$J_{SAHH} = \left(\frac{V_f^{SAHH} \times sah}{K_{SAHH}^{sah} + sah}\right) - \left(\frac{V_r^{SAHH} \times hcy}{K_{SAHH}^{hcy} + hcy}\right) \tag{4.5}$$

$$J_{MS} = \frac{V_m^{MS} \times c5mf \times hcy}{(K_{MS}^{5mf} + c5mf)(K_{MS}^{hcy} + hcy)} \tag{4.6}$$

$$J_{BHMT} = e^{-0.0021(sam+sah)} e^{0.0021(102.6)} \left(\frac{V_m^{BHMT} \times hcy \times BET}{(K_{BHMT}^{hcy} + hcy)(K_{BHMT}^{BET} + BET)}\right) \tag{4.7}$$

$$J_{CBS} = \left(\frac{V_m^{CBS} \times hcy \times cser}{(K_{CBS}^{hcy} + hcy)(K_{CBS}^{ser} + cser)}\right) \left(\frac{(1.086)(sam + sah)^2}{(30)^2 + (sam + sah)^2}\right) \tag{4.8}$$

$$J_{bMETc} = \left(\frac{V_m^{bMETc} \times bmet}{K_{bMETc} + bmet}\right) - K_{met}^{outmet} \tag{4.9}$$

$$J_{MAT1} = \left(\frac{V_m^{MAT1} \times met}{K_m^{MAT1} + met}\right) \left(0.23 + (0.8)e^{-(0.0026)(sam)}\right) \left(\frac{K_i^{MAT1} + 66.71}{K_i^{MAT1} + cgsg}\right) \tag{4.10}$$

$$J_{MAT3} = \left(\frac{V_m^{MAT1} \times (met)^{1.21}}{K_m^{MAT1} + (met)^{1.21}}\right) \left(1 + \frac{(7.2)(sam)^2}{(K_a^{MAT3})^2 + (sam)^2}\right) \left(\frac{K_i^{MAT3} + 66.71}{K_i^{MAT3} + cgsg}\right) \tag{4.11}$$

$$J_{GNMT} = \left(\frac{V_m^{GNMT} \times sam \times cgly}{(K_{GNMT}^{sam} + sam)(K_{GNMT}^{gly} + cgly)}\right) \left(\frac{1}{1 + \frac{sah}{K_i^{GNMT}}}\right) \left(\frac{4.8}{0.35 + c5mf}\right) \tag{4.12}$$

$$J_{DNMT} = \frac{V_m^{DNMT} \times sam}{K_m^{DNMT}\left(1 + \frac{sah}{K_i^{DNMT}}\right) + sam} \tag{4.13}$$

Rewriting the mass action equations explicitly, using the expressions for reaction velocities:

$$\begin{aligned}\textbf{hcy'} = &\left[\left(\frac{V_f^{SAHH}\times sah}{K_{SAHH}^{sah}+sah}\right)-\left(\frac{V_r^{SAHH}\times hcy}{K_{SAHH}^{hcy}+hcy}\right)\right]-\left[\frac{V_m^{MS}\times c5mf\times hcy}{(K_{MS}^{5mf}+c5mf)(K_{MS}^{hcy}+hcy)}\right]\\ &-\left[e^{-0.0021(sam+sah)}e^{0.0021(102.6)}\left(\frac{V_m^{BHMT}\times hcy\times BET}{(K_{BHMT}^{hcy}+hcy)(K_{BHMT}^{BET}+BET)}\right)\right]\\ &-\left[\left(\frac{V_m^{CBS}\times hcy\times cser}{(K_{CBS}^{hcy}+hcy)(K_{CBS}^{ser}+cser)}\right)\left(\frac{(1.086)(sam+sah)^2}{(30)^2+(sam+sah)^2}\right)\right]\end{aligned}\tag{4.14}$$

$$\begin{aligned}\textbf{met'} = &\left[\left(\frac{V_m^{bMETc}\times bmet}{K_{bMETc}+bmet}\right)-K_{met}^{outmet}\right]+\left[\frac{V_m^{MS}\times c5mf\times hcy}{(K_{MS}^{5mf}+c5mf)(K_{MS}^{hcy}+hcy)}\right]\\ &+\left[e^{-0.0021(sam+sah)}e^{0.0021(102.6)}\left(\frac{V_m^{BHMT}\times hcy\times BET}{(K_{BHMT}^{hcy}+hcy)(K_{BHMT}^{BET}+BET)}\right)\right]\\ &-\left[\left(\frac{V_m^{MAT1}\times met}{K_m^{MAT1}+met}\right)\left(0.23+(0.8)e^{-(0.0026)(sam)}\right)\left(\frac{K_i^{MAT1}+66.71}{K_i^{MAT1}+cgsg}\right)\right]\\ &-\left[\left(\frac{V_m^{MAT3}\times(met)^{1.21}}{K_m^{MAT3}+(met)^{1.21}}\right)\left(1+\frac{(7.2)(sam)^2}{(K_a^{MAT3})^2+(sam)^2}\right)\left(\frac{K_i^{MAT3}+66.71}{K_i^{MAT3}+cgsg}\right)\right]\end{aligned}\tag{4.15}$$

$$\begin{aligned}\textbf{sam'} = &\left[\left(\frac{V_m^{MAT1}\times met}{K_m^{MAT1}+met}\right)\left(0.23+(0.8)e^{-(0.0026)(sam)}\right)\left(\frac{K_i^{MAT1}+66.71}{K_i^{MAT1}+cgsg}\right)\right]\\ &+\left[\left(\frac{V_m^{MAT1}\times(met)^{1.21}}{K_m^{MAT1}+(met)^{1.21}}\right)\left(1+\frac{(7.2)(sam)^2}{(K_a^{MAT3})^2+(sam)^2}\right)\left(\frac{K_i^{MAT3}+66.71}{K_i^{MAT3}+cgsg}\right)\right]\\ &-\left[\left(\frac{V_m^{GNMT}\times sam\times cgly}{(K_{GNMT}^{sam}+sam)(K_{GNMT}^{gly}+cgly)}\right)\left(\frac{1}{1+\frac{sah}{K_i^{GNMT}}}\right)\left(\frac{4.8}{0.35+c5mf}\right)\right]\\ &-\left[\frac{V_m^{DNMT}\times sam}{K_m^{DNMT}\left(1+\frac{sah}{K_i^{DNMT}}\right)+sam}\right]\end{aligned}\tag{4.16}$$

$$\begin{aligned}\textbf{sah'} = &\left[\left(\frac{V_m^{GNMT}\times sam\times cgly}{(K_{GNMT}^{sam}+sam)(K_{GNMT}^{gly}+cgly)}\right)\left(\frac{1}{1+\frac{sah}{K_i^{GNMT}}}\right)\left(\frac{4.8}{0.35+c5mf}\right)\right]\\ &-\left[\frac{V_m^{DNMT}\times sam}{K_m^{DNMT}\left(1+\frac{sah}{K_i^{DNMT}}\right)+sam}\right]-\left[\left(\frac{V_f^{SAHH}\times sah}{K_{SAHH}^{sah}+sah}\right)-\left(\frac{V_r^{SAHH}\times hcy}{K_{SAHH}^{hcy}+hcy}\right)\right]\end{aligned}\tag{4.17}$$

Several constants have been used in the above expressions, the values of which are given in the table below:

Writing out the expressions after substituting the numerical values of constants:

$$\textbf{hcy'} = \left[\left(\frac{320 \times sah}{6.5 + sah}\right) - \left(\frac{4530 \times hcy}{150 + hcy}\right)\right] - \left[\frac{V_m^{MS} \times c5mf \times hcy}{(25 + c5mf)(1 + hcy)}\right] - \left[1.24043e^{-0.0021(sam+sah)}\left(\frac{2160 \times hcy \times BET}{(12 + hcy)(100 + BET)}\right)\right] - \left[\frac{1.08551\left(\frac{420000 \times hcy \times cser}{(1000+hcy)(2000+cser)}\right)}{1 + \left(\frac{900}{(sam+sah)^2}\right)}\right] \tag{4.18}$$

$$\textbf{met'} = [660 - met] + \left[\frac{V_m^{MS} \times c5mf \times hcy}{(25 + c5mf)(1 + hcy)}\right] + \left[1.24043e^{-0.0021(sam+sah)}\left(\frac{2160 \times hcy \times BET}{(12 + hcy)(100 + BET)}\right)\right] - \left[\frac{573745 \times met \times \left(0.23 + (0.8)e^{-(0.0026)(sam)}\right)}{(41 + met)(2140 + cgsg)}\right] - \left[\frac{901276 \times (met)^{1.21} \times \left(1 + \frac{7.2sam^2}{129600+sam^2}\right)}{(300 + (met)^{1.21})(4030 + cgsg)}\right] \tag{4.19}$$

$$\textbf{sam'} = \left[\frac{573745 \times met \times \left(0.23 + (0.8)e^{-(0.0026)(sam)}\right)}{(41 + met)(2140 + cgsg)}\right] + \left[\frac{901276 \times (met)^{1.21} \times \left(1 + \frac{7.2sam^2}{129600+sam^2}\right)}{(300 + (met)^{1.21})(4030 + cgsg)}\right] - \left[\frac{180 \times sam}{1.4(1 + 0.714286sah) + sam}\right] - \left[\frac{4.8\frac{260 \times sam \times cgly}{(63+sam)(130+cgly)}}{(0.35 + c5mf)(1 + \frac{sah}{18})}\right] \tag{4.20}$$

$$\textbf{sah'} = \left[\frac{180 \times sam}{1.4(1 + 0.714286sah) + sam}\right] + \left[\frac{4.8\frac{260 \times sam \times cgly}{(63+sam)(130+cgly)}}{(0.35 + c5mf)(1 + \frac{sah}{18})}\right] - \left[\left(\frac{320 \times sah}{6.5 + sah}\right) - \left(\frac{4530 \times hcy}{150 + hcy}\right)\right] \tag{4.21}$$

As can be observed in the above set of expressions, the mass action equations for Hcy, Met, SAM and SAH are dependent on the metabolites themselves, and also on bmet, BET, c5mf, cgsg, cser and cgly. The steady states of these variables, color-coded in red, which are extraneous to the **hcy-met-sam-sah** block vary with V_{max}^{MS} as shown in the following figures.

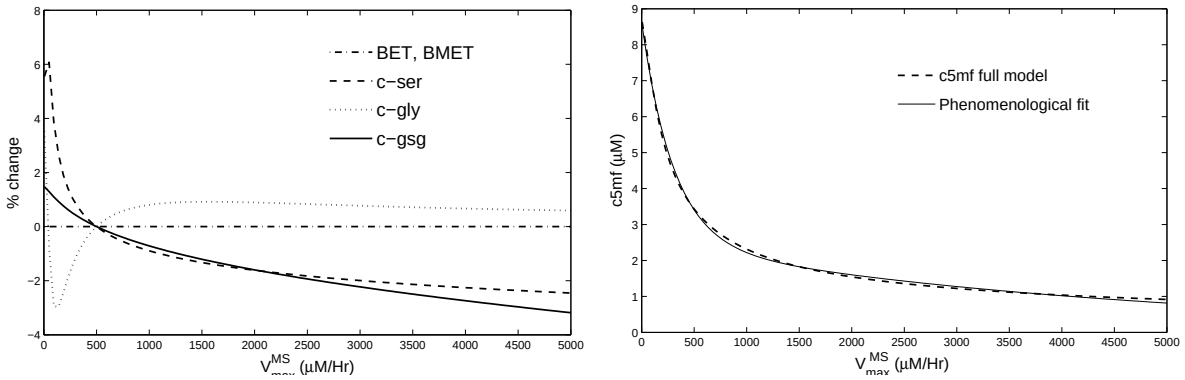

(a) (b)

Figure 4.2: Approximations and assumptions in the reduced model. (a): Percentage variation in the steady state values of BET, blood methionine (bMet), serine, glycine and glutathione disulfide with changes in the V_{max}^{MS} as seen in the Reed-Nijhout model. It can be observed that these species vary by only about 5% even with V_{max}^{MS} varying over 3 orders of magnitude justifying our assumption that these can be practically considered to be constants when studying the Methionine cycle in particular. (b): The phenomenological fit of c5mf as a function of V_{max}^{MS} as compared against the steady state values of c5mf. It can be observed that the phenomenological fit closely approximates the original behavior of c5mf values.

As can be seen from Fig. 4.2, bmet, BET, cgsg, cser and cgly do not vary much with V_{max}^{MS}. We re-wrote the mass action expressions from the Reed-Nijhout model in our reduced model by assuming these metabolites as constant parameters in our reduced model. The following values were assigned to the metabolites:

$$\textbf{cgly} = 1300 \qquad \textbf{cgsg} = 60 \qquad \textbf{cser} = 605 \qquad \textbf{BET} = 50 \qquad \textbf{bmet} = 30$$

c5mf shows significant variation with variation in the value of V_{max}^{MS}. So we fit c5mf as a phenomenological function of V_{max}^{MS} in our reduced model. The phenomenological function representing the concentration of c5mf as a function of V_m^{MS} is

$$\textbf{c5mf} = 6.141e^{-0.003301 \times V_m^{MS}} + 2.491e^{-0.0002233 \times V_m^{MS}} \tag{4.22}$$

Fig. 4.2 also shows a comparison between the steady state values of c5mf as predicted by the Reed-Nijhout model and those as calculated using the phenomenological function. It can be seen that they are in agreement with each other.

4.2 Validation

We compare the predictions computed using the reduced model with those computed using the Reed-Nijhout model, in order to validate the reduced model. Fig. 4.3 below shows a comparison between the steady state values of Hcy, Met, SAM and SAH, with

respect toV_{max}^{MS}, as computed using the Reed-Nijhout model and the reduced model.

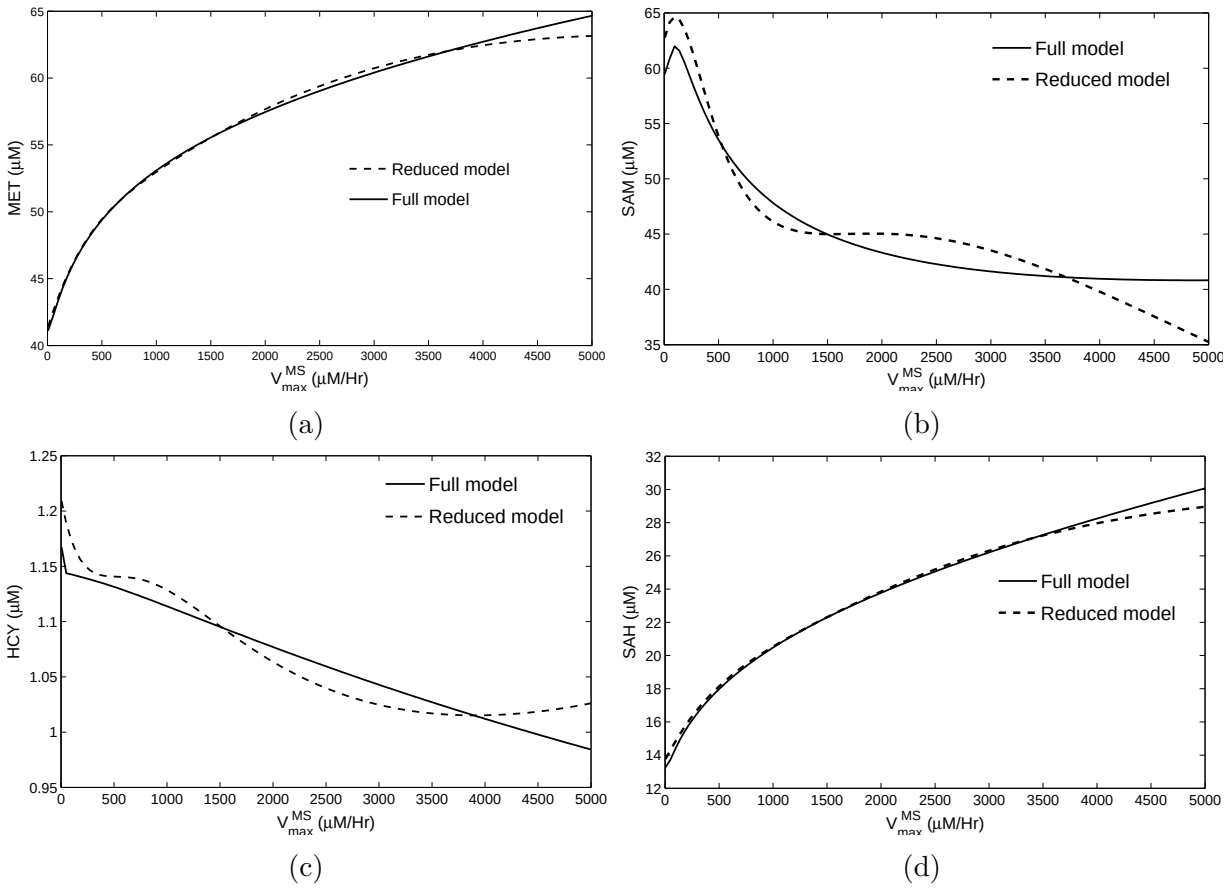

Figure 4.3: Reduced model vs Reed-Nijhout model. Steady state values of **(a):** Met, **(b):** SAM, **(c):** Hcy and **(d):** SAH calculated using the reduced model as compared with the steady state values calculated using the Reed-Nijhout model. It can be observed that the reduced model closely approximates the function of methionine cycle in the Reed-Nijhout model.

The Fig. 4.3 above shows that the reduced model is a reasonably good approximation of Reed-Nijhout model in modeling the function of the methionine cycle. Fig. 4.4 gives a numerical perspective of the information shown in Fig. 4.3. The maximum deviation from the Reed-Nijhout model is only by about 14%, further strengthening the validity of our reduced model.

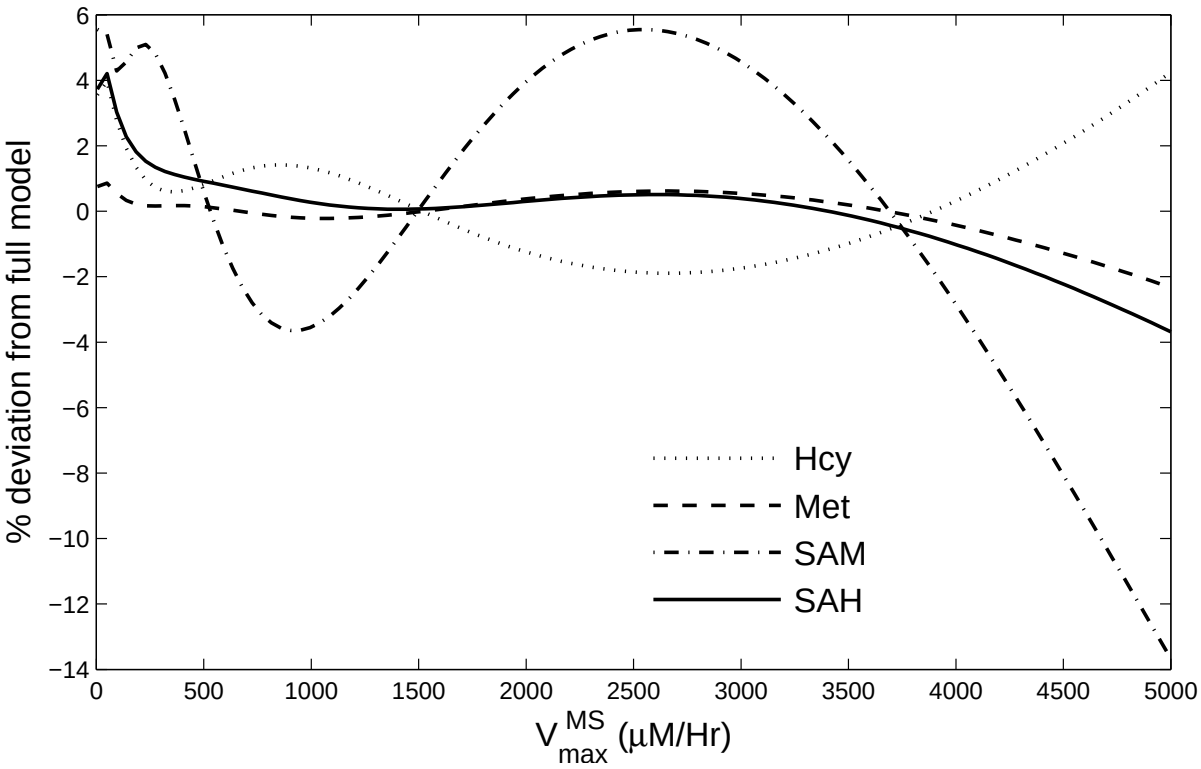

Figure 4.4: Deviation, in percentages, in the steady state values of Hcy, Met, SAM and SAH as calculated using the reduced model with respect to the steady state values calculated using the Reed-Nijhout model. It can be observed that the calculations from the reduced model deviate from those of the full well within the significant levels.

Having validated the reduced model, we focus our attention on its mass-action equations governing the metabolites in the methionine cycle. We dig deeper into the mathematical structure of these equations to explain the homeostasis of Hcy despite variation in V_{max}^{MS}. Hcy homeostasis with respect to V_{max}^{MS} is also observed in the reduced model, as shown in Fig. 4.3

Chapter 5

Implicit Differentiation

The reduced model described in the preceding chapter was built by extracting the mass action equations pertaining to the methionine cycle from the Reed-Nijhout model and approximating the fluxes connecting the methionine cycle with the rest of the network.

Re-writing the mass-action equations after substituting the constant values of the extraneous fluxes, and the phenomenological function for c5mf, they look as shown below:

$$\begin{aligned}\textbf{hcy'} = {} & \frac{320 \times sah}{6.5 + sah} - \frac{4530 \times hcy}{150 + hcy} - \frac{7.18532 \times 10^{11} \times hcy}{(1000 + hcy)(1 + \frac{900}{(sah+sam)^2)}} - \frac{893.11 \times e^{-0.0021(sah+sam)} \times hcy}{12 + hcy} \\ & - \frac{6.141e^{(-0.003301 \times V_m^{MS}} + 2.491e^{-0.0002233 \times V_m^{MS}}) \times V_m^{MS} \times hcy}{25 + 6.141e^{(-0.003301 \times V_m^{MS}} + 2.491e^{-0.0002233 \times V_m^{MS}}) \times (1 + hcy)} \end{aligned} \tag{5.1}$$

$$\begin{aligned}\textbf{met'} = {} & 660 - met + \frac{6.141e^{(-0.003301 \times V_m^{MS}} + 2.491e^{-0.0002233 \times V_m^{MS}}) \times V_m^{MS} \times hcy}{25 + 6.141e^{(-0.003301 \times V_m^{MS}} + 2.491e^{-0.0002233 \times V_m^{MS}}) \times (1 + hcy)} \\ & + \frac{893.11 \times e^{-0.0021(sah+sam)} \times hcy}{12 + hcy} - \frac{114749 \times (0.23 + 0.8e^{-0.0026sam}) \times met}{440 \times (41 + met)} \\ & - \frac{450638 \times met^{1.21} \times \left(1 + \frac{7.2 \times sam^2}{129600 + sam^2}\right)}{2045 \times (300 + met^{1.21})} \end{aligned} \tag{5.2}$$

$$\begin{aligned}\textbf{sam'} = {} & \frac{114749 \times (0.23 + 0.8e^{-0.0026sam}) \times met}{440 \times (41 + met)} \\ & - \frac{1134.55 \times sam}{\left[(0.35 + 6.141e^{(-0.003301 \times V_m^{MS}} + 2.491e^{-0.0002233 \times V_m^{MS})})(1 + \frac{sah}{18})(63 + sam)\right]} \\ & - \frac{180 \times sam}{1.4(1 + 0.714286 \times sah) + sam} + \frac{450638 \times met^{1.21} \times \left(1 + \frac{7.2 \times sam^2}{129600 + sam^2}\right)}{2045 \times (300 + met^{1.21})} \end{aligned} \tag{5.3}$$

$$\textbf{sah'} = \frac{4530 \times hcy}{150 + hcy} - \frac{320 \times sah}{6.5 + sah} + \frac{1134.55 \times sam}{\left[(0.35 + 6.141e^{(-0.003301 \times V_m^{MS}} + 2.491e^{-0.0002233 \times V_m^{MS}})(1 + \frac{sah}{18})(63 + sam)\right]} + \frac{180 \times sam}{1.4(1 + 0.714286 \times sah) + sam} \tag{5.4}$$

We tried to investigate the homeostasis of Hcy by differentiating the steady state expressions for the metabolites, with respect to V_{max}^{MS}. The L.H.S of the mass-action equations were set to zero to derive the steady state expressions for the metabolites. The steady state values of the metabolites as functions of V_{max}^{MS} are color-coded blue.

$$0 = \frac{320 \times sah^*(V_m^{MS})}{6.5 + sah^*(V_m^{MS})} - \frac{4530 \times hcy^*(V_m^{MS})}{150 + hcy^*(V_m^{MS})} - \frac{7.18532 \times 10^{11} \times hcy^*(V_m^{MS})}{(1000 + hcy^*(V_m^{MS}))(1 + \frac{900}{(sah^*(V_m^{MS}) + sam^*(V_m^{MS}))^2)}} - \frac{893.11 \times e^{-0.0021(sah^*(V_m^{MS}) + sam^*(V_m^{MS}))} \times hcy^*(V_m^{MS})}{12 + hcy^*(V_m^{MS})} - \frac{6.141e^{(-0.003301 \times V_m^{MS}} + 2.491e^{-0.0002233 \times V_m^{MS}}) \times V_m^{MS} \times hcy^*(V_m^{MS})}{25 + 6.141e^{(-0.003301 \times V_m^{MS}} + 2.491e^{-0.0002233 \times V_m^{MS}}) \times (1 + hcy^*(V_m^{MS}))} \tag{5.5}$$

$$0 = 660 - met^*(V_m^{MS}) + \frac{6.141e^{(-0.003301 \times V_m^{MS}} + 2.491e^{-0.0002233 \times V_m^{MS}}) \times V_m^{MS} \times hcy^*(V_m^{MS})}{25 + 6.141e^{(-0.003301 \times V_m^{MS}} + 2.491e^{-0.0002233 \times V_m^{MS}}) \times (1 + hcy^*(V_m^{MS}))} + \frac{893.11 \times e^{-0.0021(sah^*(V_m^{MS}) + sam^*(V_m^{MS}))} \times hcy^*(V_m^{MS})}{12 + hcy^*(V_m^{MS})} - \frac{114749 \times (0.23 + 0.8e^{-0.0026 sam^*(V_m^{MS})}) \times met^*(V_m^{MS})}{440 \times (41 + met^*(V_m^{MS}))} - \frac{450638 \times met^*(V_m^{MS})^{1.21} \times \left(1 + \frac{7.2 \times sam^*(V_m^{MS})^2}{129600 + sam^*(V_m^{MS})^2}\right)}{2045 \times (300 + met^*(V_m^{MS})^{1.21})} \tag{5.6}$$

$$0 = \frac{114749 \times (0.23 + 0.8e^{-0.0026 sam^*(V_m^{MS})}) \times met^*(V_m^{MS})}{440 \times (41 + met^*(V_m^{MS}))} - \frac{1134.55 \times sam^*(V_m^{MS})}{\left[(0.35 + 6.141e^{(-0.003301 \times V_m^{MS}} + 2.491e^{-0.0002233 \times V_m^{MS}})(1 + \frac{sah^*(V_m^{MS})}{18})(63 + sam^*(V_m^{MS}))\right]} - \frac{180 \times sam^*(V_m^{MS})}{1.4(1 + 0.714286 \times sah^*(V_m^{MS})) + sam^*(V_m^{MS})} + \frac{450638 \times met^*(V_m^{MS})^{1.21} \times \left(1 + \frac{7.2 \times sam^*(V_m^{MS})^2}{129600 + sam^*(V_m^{MS})^2}\right)}{2045 \times (300 + met^*(V_m^{MS})^{1.21})} \tag{5.7}$$

$$0 = \frac{4530 \times hcy^*(V_m^{MS})}{150 + hcy^*(V_m^{MS})} - \frac{320 \times sah^*(V_m^{MS})}{6.5 + sah^*(V_m^{MS})} + \frac{180 \times sam^*(V_m^{MS})}{1.4(1 + 0.714286 \times sah^*(V_m^{MS})) + sam^*(V_m^{MS})} + \frac{1134.55 \times sam^*(V_m^{MS})}{\left[(0.35 + 6.141e^{(-0.003301 \times V_m^{MS}} + 2.491e^{-0.0002233 \times V_m^{MS}})(1 + \frac{sah^*(V_m^{MS})}{18})(63 + sam^*(V_m^{MS}))\right]} \tag{5.8}$$

Here $sah^*(V_m^{MS})$ refers to the steady state value of SAH as a function of V_{max}^{MS}. We implicitly differentiate the above expressions with respect to V_{max}^{MS} to examine the effect of changes in V_{max}^{MS} on the steady state values. We end up with:

$$
\begin{aligned}
0 = & \frac{7.18532 \times 10^{11} hcy^*(V_m^{MS}) hcy^{*\prime}(V_m^{MS})}{(hcy^*(V_m^{MS}) + 1000)^2 \left(\frac{900}{(sah^*(V_m^{MS}) + sam^*(V_m^{MS}))^2} + 1\right)} \\
& + \frac{893.11 hcy^*(V_m^{MS}) hcy^{*\prime}(V_m^{MS}) e^{-0.0021(sah^*(V_m^{MS}) + sam^*(V_m^{MS}))}}{(hcy^*(V_m^{MS}) + 12)^2} \\
& - \frac{893.11 hcy^{*\prime}(V_m^{MS}) e^{-0.0021(sah^*(V_m^{MS}) + sam^*(V_m^{MS}))}}{hcy^*(V_m^{MS}) + 12} \\
& - \frac{7.18532 \times 10^{11} hcy^{*\prime}(V_m^{MS})}{(hcy^*(V_m^{MS}) + 1000) \left(\frac{900}{(sah^*(V_m^{MS}) + sam^*(V_m^{MS}))^2} + 1\right)} \\
& + \frac{\left(6.141 e^{-0.003301 V_m^{MS}} + 2.491 e^{-0.0002233 V_m^{MS}}\right) V_m^{MS} hcy^*(V_m^{MS}) hcy^{*\prime}(V_m^{MS})}{\left(6.141 e^{-0.003301 V_m^{MS}} + 2.491 e^{-0.0002233 V_m^{MS}} + 25\right) (hcy^*(V_m^{MS}) + 1)^2} \\
& + \frac{4530 hcy^*(V_m^{MS}) hcy^{*\prime}(V_m^{MS})}{(hcy^*(V_m^{MS}) + 150)^2} \\
& - \frac{\left(6.141 e^{-0.003301 V_m^{MS}} + 2.491 e^{-0.0002233 V_m^{MS}}\right) V_m^{MS} hcy^{*\prime}(V_m^{MS})}{\left(6.141 e^{-0.003301 V_m^{MS}} + 2.491 e^{-0.0002233 V_m^{MS}} + 25\right) (hcy^*(V_m^{MS}) + 1)} \\
& - \frac{4530 hcy^{*\prime}(V_m^{MS})}{hcy^*(V_m^{MS}) + 150} \\
& + \frac{1.87553 hcy^*(V_m^{MS}) e^{-0.0021(sah^*(V_m^{MS}) + sam^*(V_m^{MS}))} \left(sah^{*\prime}(V_m^{MS}) + sam^{*\prime}(V_m^{MS})\right)}{hcy^*(V_m^{MS}) + 12} \\
& - \frac{1.29336 \times 10^{15} hcy^*(V_m^{MS}) \left(sah^{*\prime}(V_m^{MS}) + sam^{*\prime}(V_m^{MS})\right)}{(hcy^*(V_m^{MS}) + 1000)(sah^*(V_m^{MS}) + sam^*(V_m^{MS}))^3 \left(\frac{900}{(sah^*(V_m^{MS}) + sam^*(V_m^{MS}))^2} + 1\right)^2} \\
& - \frac{\left(-0.0202714 e^{-0.003301 V_m^{MS}} - 0.00055624 e^{-0.0002233 V_m^{MS}}\right) V_m^{MS} hcy^*(V_m^{MS})}{\left(6.141 e^{-0.003301 V_m^{MS}} + 2.491 e^{-0.0002233 V_m^{MS}} + 25\right) (hcy^*(V_m^{MS}) + 1)} \\
& + \frac{\left(-0.0202714 e^{-0.003301 V_m^{MS}} - 0.00055624 e^{-0.0002233 V_m^{MS}}\right) V_m^{MS}}{\left(6.141 e^{-0.003301 V_m^{MS}} + 2.491 e^{-0.0002233 V_m^{MS}} + 25\right)^2 (hcy^*(V_m^{MS}) + 1)} \times \\
& \left(6.141 e^{-0.003301 V_m^{MS}} + 2.491 e^{-0.0002233 V_m^{MS}}\right) hcy^*(V_m^{MS}) \\
& - \frac{\left(6.141 e^{-0.003301 V_m^{MS}} + 2.491 e^{-0.0002233 V_m^{MS}}\right) hcy^*(V_m^{MS})}{\left(6.141 e^{-0.003301 V_m^{MS}} + 2.491 e^{-0.0002233 V_m^{MS}} + 25\right) (hcy^*(V_m^{MS}) + 1)} \\
& + \frac{320 sah^{*\prime}(V_m^{MS})}{sah^*(V_m^{MS}) + 6.5} \\
& - \frac{320 sah^*(V_m^{MS}) sah^{*\prime}(V_m^{MS})}{(sah^*(V_m^{MS}) + 6.5)^2}
\end{aligned}
\tag{5.9}
$$

$$
\begin{aligned}
0 = & \frac{114749 met^*(V_m^{MS}) \left(0.23 + 0.8 e^{-0.0026 sam^*(V_m^{MS})}\right) met^{*\prime}(V_m^{MS})}{440 (met^*(V_m^{MS}) + 41)^2} \\
& - \frac{114749 \left(0.23 + 0.8 e^{-0.0026 sam^*(V_m^{MS})}\right) met^{*\prime}(V_m^{MS})}{440 (met^*(V_m^{MS}) + 41)} \\
& + \frac{893.11 hcy^{*\prime}(V_m^{MS}) e^{-0.0021 (sah^*(V_m^{MS}) + sam^*(V_m^{MS}))}}{hcy^*(V_m^{MS}) + 12} \\
& - \frac{893.11 hcy^*(V_m^{MS}) hcy^{*\prime}(V_m^{MS}) e^{-0.0021 (sah^*(V_m^{MS}) + sam^*(V_m^{MS}))}}{(hcy^*(V_m^{MS}) + 12)^2} \\
& + \frac{\left(6.141 e^{-0.003301 V_m^{MS}} + 2.491 e^{-0.0002233 V_m^{MS}}\right) V_m^{MS} hcy^{*\prime}(V_m^{MS})}{\left(6.141 e^{-0.003301 V_m^{MS}} + 2.491 e^{-0.0002233 V_m^{MS}} + 25\right) (hcy^*(V_m^{MS}) + 1)} \\
& - \frac{\left(6.141 e^{-0.003301 V_m^{MS}} + 2.491 e^{-0.0002233 V_m^{MS}}\right) V_m^{MS} hcy^*(V_m^{MS}) hcy^{*\prime}(V_m^{MS})}{\left(6.141 e^{-0.003301 V_m^{MS}} + 2.491 e^{-0.0002233 V_m^{MS}} + 25\right) (hcy^*(V_m^{MS}) + 1)^2} \\
& - \frac{1.87553 hcy^*(V_m^{MS}) e^{-0.0021 (sah^*(V_m^{MS}) + sam^*(V_m^{MS}))} \left(sah^{*\prime}(V_m^{MS}) + sam^{*\prime}(V_m^{MS})\right)}{hcy^*(V_m^{MS}) + 12} \\
& + \frac{\left(-0.0202714 e^{-0.003301 V_m^{MS}} - 0.00055624 e^{-0.0002233 V_m^{MS}}\right) V_m^{MS} hcy^*(V_m^{MS})}{\left(6.141 e^{-0.003301 V_m^{MS}} + 2.491 e^{-0.0002233 V_m^{MS}} + 25\right) (hcy^*(V_m^{MS}) + 1)} \\
& - \frac{\left(-0.0202714 e^{-0.003301 V_m^{MS}} - 0.00055624 e^{-0.0002233 V_m^{MS}}\right) hcy^*(V_m^{MS})}{\left(6.141 e^{-0.003301 V_m^{MS}} + 2.491 e^{-0.0002233 V_m^{MS}} + 25\right)^2 (hcy^*(V_m^{MS}) + 1)} \times \\
& \left(6.141 e^{-0.003301 V_m^{MS}} + 2.491 e^{-0.0002233 V_m^{MS}}\right) V_m^{MS} \\
& + \frac{\left(6.141 e^{-0.003301 V_m^{MS}} + 2.491 e^{-0.0002233 V_m^{MS}}\right) hcy^*(V_m^{MS})}{\left(6.141 e^{-0.003301 V_m^{MS}} + 2.491 e^{-0.0002233 V_m^{MS}} + 25\right) (hcy^*(V_m^{MS}) + 1)} \\
& + \frac{266.637 met^*(V_m^{MS})^{1.42} \left(\frac{7.2 sam^*(V_m^{MS})^2}{sam^*(V_m^{MS})^2 + 129600} + 1\right) met^{*\prime}(V_m^{MS})}{\left(met^*(V_m^{MS})^{1.21} + 300\right)^2} \\
& - \frac{266.637 met^*(V_m^{MS})^{0.21} \left(\frac{7.2 sam^*(V_m^{MS})^2}{sam^*(V_m^{MS})^2 + 129600} + 1\right) met^{*\prime}(V_m^{MS})}{met^*(V_m^{MS})^{1.21} + 300} \\
& - met^{*\prime}(V_m^{MS}) \\
& - \frac{450638 met^*(V_m^{MS})^{1.21} \left(\frac{14.4 sam^*(V_m^{MS}) sam^{*\prime}(V_m^{MS})}{sam^*(V_m^{MS})^2 + 129600} - \frac{14.4 sam^*(V_m^{MS})^3 sam^{*\prime}(V_m^{MS})}{\left(sam^*(V_m^{MS})^2 + 129600\right)^2}\right)}{2045 \left(met^*(V_m^{MS})^{1.21} + 300\right)} \\
& + \frac{0.54245 met^*(V_m^{MS}) e^{-0.0026 sam^*(V_m^{MS})} sam^{*\prime}(V_m^{MS})}{met^*(V_m^{MS}) + 41}
\end{aligned}
\tag{5.10}
$$

$$
\begin{aligned}
0 = &- \frac{114749 met^*(V_m^{MS}) \left(0.23 + 0.8 e^{-0.0026 sam^*(V_m^{MS})}\right) met^{*\prime}(V_m^{MS})}{440 (met^*(V_m^{MS}) + 41)^2} \\
&+ \frac{114749 \left(0.23 + 0.8 e^{-0.0026 sam^*(V_m^{MS})}\right) met^{*\prime}(V_m^{MS})}{440 (met^*(V_m^{MS}) + 41)} \\
&+ \frac{63.0303 sam^*(V_m^{MS}) sah^{*\prime}(V_m^{MS})}{\left(0.35 + 6.141 e^{-0.003301 V_m^{MS}} + 2.491 e^{-0.0002233 V_m^{MS}}\right) \left(\frac{sah^*(V_m^{MS})}{18} + 1\right)^2 (sam^*(V_m^{MS}) + 63)} \\
&- \frac{1134.55 sam^{*\prime}(V_m^{MS})}{\left(0.35 + 6.141 e^{-0.003301 V_m^{MS}} + 2.491 e^{-0.0002233 V_m^{MS}}\right) \left(\frac{sah^*(V_m^{MS})}{18} + 1\right) (sam^*(V_m^{MS}) + 63)} \\
&+ \frac{1134.55 sam^*(V_m^{MS}) sam^{*\prime}(V_m^{MS})}{\left(0.35 + 6.141 e^{-0.003301 V_m^{MS}} + 2.491 e^{-0.0002233 V_m^{MS}}\right) \left(\frac{sah^*(V_m^{MS})}{18} + 1\right) (sam^*(V_m^{MS}) + 63)^2} \\
&+ \frac{1134.55 \left(-0.0202714 e^{-0.003301 V_m^{MS}} - 0.00055624 e^{-0.0002233 V_m^{MS}}\right) sam^*(V_m^{MS})}{\left(0.35 + 6.141 e^{-0.003301 V_m^{MS}} + 2.491 e^{-0.0002233 V_m^{MS}}\right)^2 \left(\frac{sah^*(V_m^{MS})}{18} + 1\right) (sam^*(V_m^{MS}) + 63)} \\
&- \frac{266.637 met^*(V_m^{MS})^{1.42} \left(\frac{7.2 sam^*(V_m^{MS})^2}{sam^*(V_m^{MS})^2 + 129600} + 1\right) met^{*\prime}(V_m^{MS})}{\left(met^*(V_m^{MS})^{1.21} + 300\right)^2} \\
&+ \frac{266.637 met^*(V_m^{MS})^{0.21} \left(\frac{7.2 sam^*(V_m^{MS})^2}{sam^*(V_m^{MS})^2 + 129600} + 1\right) met^{*\prime}(V_m^{MS})}{met^*(V_m^{MS})^{1.21} + 300} \\
&+ \frac{450638 met^*(V_m^{MS})^{1.21} \left(\frac{14.4 sam^*(V_m^{MS}) sam^{*\prime}(V_m^{MS})}{sam^*(V_m^{MS})^2 + 129600} - \frac{14.4 sam^*(V_m^{MS})^3 sam^{*\prime}(V_m^{MS})}{\left(sam^*(V_m^{MS})^2 + 129600\right)^2}\right)}{2045 \left(met^*(V_m^{MS})^{1.21} + 300\right)} \\
&- \frac{0.54245 met^*(V_m^{MS}) e^{-0.0026 sam^*(V_m^{MS})} sam^{*\prime}(V_m^{MS})}{met^*(V_m^{MS}) + 41} \\
&+ \frac{180 sam^*(V_m^{MS}) \left(1. sah^{*\prime}(V_m^{MS}) + sam^{*\prime}(V_m^{MS})\right)}{(1.4(0.714286 sah^*(V_m^{MS}) + 1) + sam^*(V_m^{MS}))^2} \\
&- \frac{180 sam^{*\prime}(V_m^{MS})}{1.4(0.714286 sah^*(V_m^{MS}) + 1) + sam^*(V_m^{MS})}
\end{aligned}
\tag{5.11}
$$

$$
\begin{aligned}
0 = & \frac{7.18532 \times 10^{11} hcy^*(V_m^{MS}) hcy^{*\prime}(V_m^{MS})}{(hcy^*(V_m^{MS}) + 1000)^2 \left(\frac{900}{(sah^*(V_m^{MS}) + sam^*(V_m^{MS}))^2} + 1\right)} \\
& + \frac{893.11 hcy^*(V_m^{MS}) hcy^{*\prime}(V_m^{MS}) e^{-0.0021(sah^*(V_m^{MS}) + sam^*(V_m^{MS}))}}{(hcy^*(V_m^{MS}) + 12)^2} \\
& - \frac{893.11 hcy^{*\prime}(V_m^{MS}) e^{-0.0021(sah^*(V_m^{MS}) + sam^*(V_m^{MS}))}}{hcy^*(V_m^{MS}) + 12} \\
& - \frac{7.18532 \times 10^{11} hcy^{*\prime}(V_m^{MS})}{(hcy^*(V_m^{MS}) + 1000) \left(\frac{900}{(sah^*(V_m^{MS}) + sam^*(V_m^{MS}))^2} + 1\right)} \\
& + \frac{\left(6.141 e^{-0.003301 V_m^{MS}} + 2.491 e^{-0.0002233 V_m^{MS}}\right) V_m^{MS} hcy^*(V_m^{MS}) hcy^{*\prime}(V_m^{MS})}{\left(6.141 e^{-0.003301 V_m^{MS}} + 2.491 e^{-0.0002233 V_m^{MS}} + 25\right) (hcy^*(V_m^{MS}) + 1)^2} \\
& + \frac{4530 hcy^*(V_m^{MS}) hcy^{*\prime}(V_m^{MS})}{(hcy^*(V_m^{MS}) + 150)^2} \\
& - \frac{\left(6.141 e^{-0.003301 V_m^{MS}} + 2.491 e^{-0.0002233 V_m^{MS}}\right) V_m^{MS} hcy^{*\prime}(V_m^{MS})}{\left(6.141 e^{-0.003301 V_m^{MS}} + 2.491 e^{-0.0002233 V_m^{MS}} + 25\right) (hcy^*(V_m^{MS}) + 1)} \\
& - \frac{4530 hcy^{*\prime}(V_m^{MS})}{hcy^*(V_m^{MS}) + 150} \\
& + \frac{1.87553 hcy^*(V_m^{MS}) e^{-0.0021(sah^*(V_m^{MS}) + sam^*(V_m^{MS}))} \left(sah^{*\prime}(V_m^{MS}) + sam^{*\prime}(V_m^{MS})\right)}{hcy^*(V_m^{MS}) + 12} \\
& - \frac{1.29336 \times 10^{15} hcy^*(V_m^{MS}) \left(sah^{*\prime}(V_m^{MS}) + sam^{*\prime}(V_m^{MS})\right)}{(hcy^*(V_m^{MS}) + 1000)(sah^*(V_m^{MS}) + sam^*(V_m^{MS}))^3 \left(\frac{900}{(sah^*(V_m^{MS}) + sam^*(V_m^{MS}))^2} + 1\right)^2} \\
& - \frac{\left(-0.0202714 e^{-0.003301 V_m^{MS}} - 0.00055624 e^{-0.0002233 V_m^{MS}}\right) V_m^{MS} hcy^*(V_m^{MS})}{\left(6.141 e^{-0.003301 V_m^{MS}} + 2.491 e^{-0.0002233 V_m^{MS}} + 25\right) (hcy^*(V_m^{MS}) + 1)} \\
& + \frac{\left(-0.0202714 e^{-0.003301 V_m^{MS}} - 0.00055624 e^{-0.0002233 V_m^{MS}}\right) hcy^*(V_m^{MS})}{\left(6.141 e^{-0.003301 V_m^{MS}} + 2.491 e^{-0.0002233 V_m^{MS}} + 25\right)^2 (hcy^*(V_m^{MS}) + 1)} \times \\
& \left(6.141 e^{-0.003301 V_m^{MS}} + 2.491 e^{-0.0002233 V_m^{MS}}\right) V_m^{MS} \\
& - \frac{\left(6.141 e^{-0.003301 V_m^{MS}} + 2.491 e^{-0.0002233 V_m^{MS}}\right) hcy^*(V_m^{MS})}{\left(6.141 e^{-0.003301 V_m^{MS}} + 2.491 e^{-0.0002233 V_m^{MS}} + 25\right) (hcy^*(V_m^{MS}) + 1)} \\
& + \frac{320 sah^{*\prime}(V_m^{MS})}{sah^*(V_m^{MS}) + 6.5} \\
& - \frac{320 sah^*(V_m^{MS}) sah^{*\prime}(V_m^{MS})}{(sah^*(V_m^{MS}) + 6.5)^2}
\end{aligned}
\tag{5.12}
$$

We tried to derive steady state expressions for each of the metabolites in the methionine cycle using the equations above. Their cumbersome nature rendered them inconvenient for any analysis, even by powerful mathematical softwares like Wolfram Mathematica®. These equations do not shed much light on the dependence of Hcy

steady state values on V_{max}^{MS}. To go around this problem, we build a stylized model to qualitatively study the topology of the methionine cycle.

Chapter 6

Stylized Model

In a preceding chapter we built a reduced model approximating the function of the methionine cycle by extracting the relevant parts from the Reed-Nijhout model. In order to understand the mathematics behind the reduced model, we build a simplistic motif that approximates the topology of the reduced model. We will refer to this simplistic motif as the "Stylized model" henceforth.

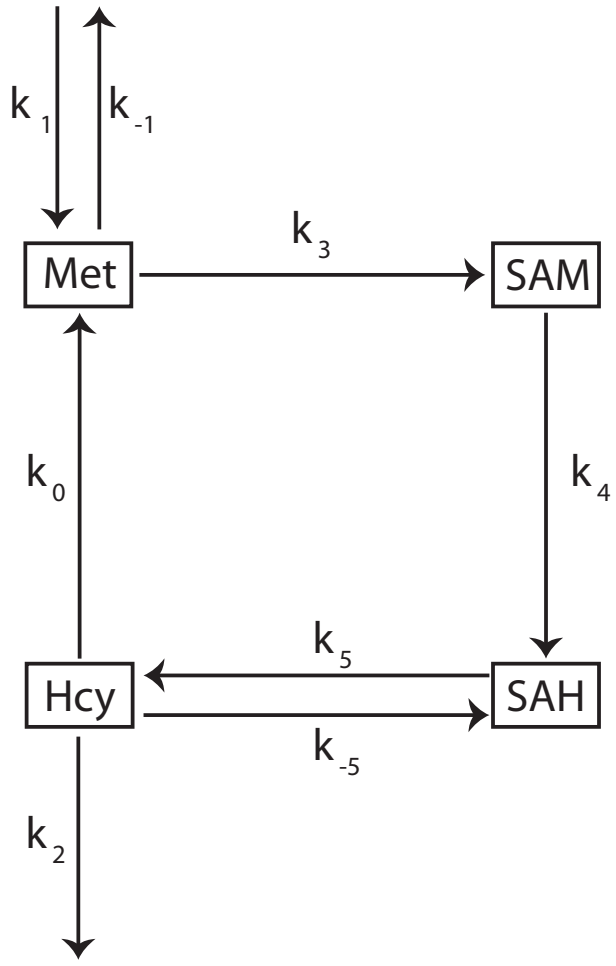

Figure 6.1: Stylized model built to approximate the topology of the reduced model (Fig. 4.1).

The constant flux from blood methionine into Met is shown as k_1 and the Met-dependent backward flux into the blood is assumed to be regulated by a single rate constant k_{-1}. Enzymes MAT1 and MAT3 regulate the flux from Met to SAM in the reduced model which is shown to be regulated by the rate constant k_3 in the stylized model. k_4 is taken to be the rate constant for the flux originally regulated by enzymes GNMT and DNMT in the reduced model. k_5 regulates the forward flux from SAH to Hcy and k_{-5} the backward flux, both of which are due to SAHH in the reduced model. The rate constant k_2 regulates the flux from Hcy into the cystathionine residues and k_0 replaces the regulation due to enzymes MS and BHMT from Hcy to Met.

This stylized model was built only to gain an insight into the topology of the methionine cycle. The stylized model is not meant to predict the steady states of the metabolites constituting the methionine cycle. Hence, we have not shown any comparisons of the steady state plots as predicted by the stylized model with those of the reduced model or the Reed-Nijhout model.

6.1 Mass-action Equations

The mass action equations for the stylized model depicted in the Fig. 6.1 are as follows:

$$\mathbf{hcy'} = k_4\ sah - k_5\ hcy - k_1\ hcy - k_6\ hcy \tag{6.1}$$
$$\mathbf{met'} = k_3\ sam - k_4\ sah + k_5\ hcy \tag{6.2}$$
$$\mathbf{sam'} = k_2\ met - k_3\ sam \tag{6.3}$$
$$\mathbf{sah'} = k + k_1\ hcy - k_7\ met - k_2\ met \tag{6.4}$$

The steady state expressions for the above set of differential equations is

$$hcy^* = \frac{k\ k_2}{k_2\ k_6 + k_1\ k_7 + k_6\ k_7} \tag{6.5}$$
$$met^* = \frac{k\ (k_1 + k_6)}{k_2\ k_6 + k_1\ k_7 + k_6\ k_7} \tag{6.6}$$
$$sam^* = \frac{k\ k_2(k_1 + k_6)}{k_3\ (k_2\ k_6 + k_1\ k_7 + k_6\ k_7)} \tag{6.7}$$
$$sah^* = \frac{k\ k_2\ (k_1 + k_5 + k_6)}{k_4\ (k_2\ k_6 + k_1\ k_7 + k_6\ k_7)} \tag{6.8}$$

Since k_1 is the rate constant approximating the flux due to MS and BHMT, we differentiate the above equations with respect to k_1,

$$\frac{dhcy^*}{dk_1} = -\frac{k\ k_2\ k_7}{(k_2\ k_6 + k_1\ k_7 + k_6\ k_7)^2} \tag{6.9}$$

$$\frac{dmet^*}{dk_1} = -\frac{k(k_1 + k_6)k_7}{(k_2\ k_6 + k_1\ k_7 + k_6\ k_7)^2} + \frac{k}{(k_2\ k_6 + k_1\ k_7 + k_6\ k_7)} \tag{6.10}$$

$$\frac{dsam^*}{dk_1} = -\frac{k\ k_2(k_1 + k_6)k_7}{k_3(k_2\ k_6 + k_1\ k_7 + k_6\ k_7)^2} + \frac{k\ k_2}{k_3(k_2\ k_6 + k_1\ k_7 + k_6\ k_7)} \tag{6.11}$$

$$\frac{dsah^*}{dk_1} = -\frac{k\ k_2(k_1 + k_5 + k_6)k_7}{k_4(k_2\ k_6 + k_1\ k_7 + k_6\ k_7)^2} + \frac{k\ k_2}{k_4(k_2\ k_6 + k_1\ k_7 + k_6\ k_7)} \tag{6.12}$$

As can be observed in the above expressions, the steady state value of Hcy is dependent on the value of k_1 through a term in the denominator. k_1 is by being multiplied to k_7. A smaller value of k_7 leads to a weaker effect of changes in k_1 on the steady state value of Hcy. k_7 corresonds to the parameter k_{met}^{outmet} in our reduced model. This leads us to hypothesize that k_{met}^{outmet} controls the Hcy buffering capacity. We test this hypothesis in the subsequent chapter.

Chapter 7

Hyperhomocysteinemia in the model

In this chapter we test the hypothesis that the value of the parameter k_{met}^{outmet} is critical in explaining the homeostatic behavior of Hcy despite huge variation in V_{max}^{MS}. We also verify another mechanism known to lead to hyperhomocysteinemia – inhibition of CBS. Naively looking at the Reed-Nijhout model (shown in the appendix) one is led to believe that an increase in Hcy levels should percolate downstream and result in increased GSH levels. We try to test this hypothesis by artificially turning up the concentration of Hcy in the Reed-Nijhout model and keeping all other parameters the same.

7.1 k_{met}^{outmet} is critical to Hcy homeostasis

In order to test the hypothesis that k_{met}^{outmet} holds the key to Hcy homeostasis, we vary the value of k_{met}^{outmet} in the reduced model and the Reed-Nijhout model.

We varied the value of k_{met}^{outmet} by over three orders of magnitude. k_{met}^{outmet} was originally assigned a value of 1 μM/Hr in the models. Fig. 7.1 below shows the effect of amplifying the value of k_{met}^{outmet} on the buffering capacity of Hcy.

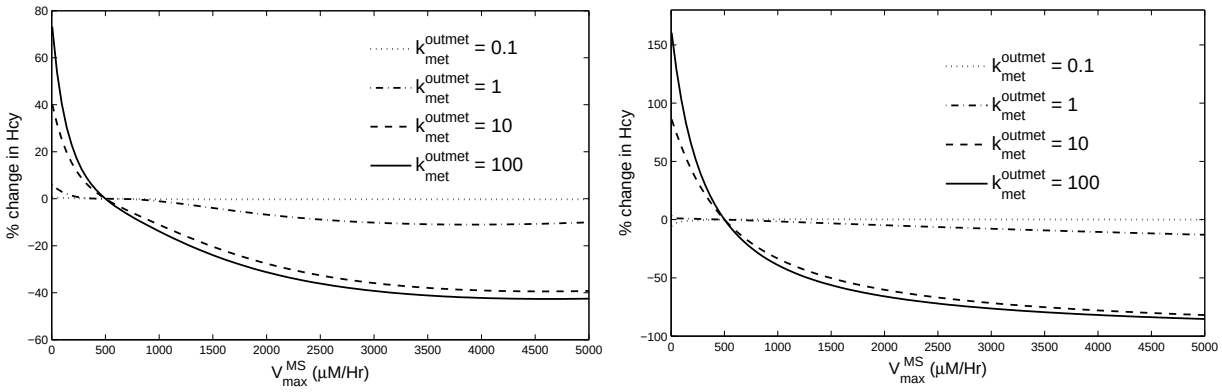

(a) (b)

Figure 7.1: Steady states of Hcy are effected by k_{met}^{outmet}. Fig.(a) shows variation in the Hcy steady states, in the reduced model, plotted against V_{max}^{MS} . **(b)** shows variation in the Hcy steady states, in the Reed-Nijhout model, plotted against V_{max}^{MS} . Hcy steady state at V_{max}^{MS} =500, for each value of k_{met}^{outmet}, is considered the baseline value for calculating the variation. Please note that the vertical axes are different for the figures. This confirms our prediction that k_{met}^{outmet} controls the Hcy buffering capacity. Higher value of k_{met}^{outmet} leads to a larger variation in the Hcy steady states.

As can be observed from the Fig. 7.1 above, varying the value of k_{met}^{outmet} significantly affects the buffering capacity of Hcy. In view of this observation, we theorize that vitamin B_{12} deficiency could be affecting the value of k_{met}^{outmet} leading to hyperhomocysteinemia in the model.

7.2 CBS inhibition leads to hyperhomocysteinemia in the model

CBS is a co-enzyme of vitamin B_6 that catalyzes the conversion of Hcy into cystathionine. Vitamin B_6 is also known to lead to severe hyperhomocysteinemia [7], primarily explained due to inhibition of CBS activity, leading to piling up Hcy levels.

We inhibit the CBS activity in Reed-Nijhout model by varying the value of V_{CBS}^{max}. Fig. 7.2 shows that the Hcy values rise phenomenally as expected. We also observe falling GSH values, explained by lack of cystathionine supply.

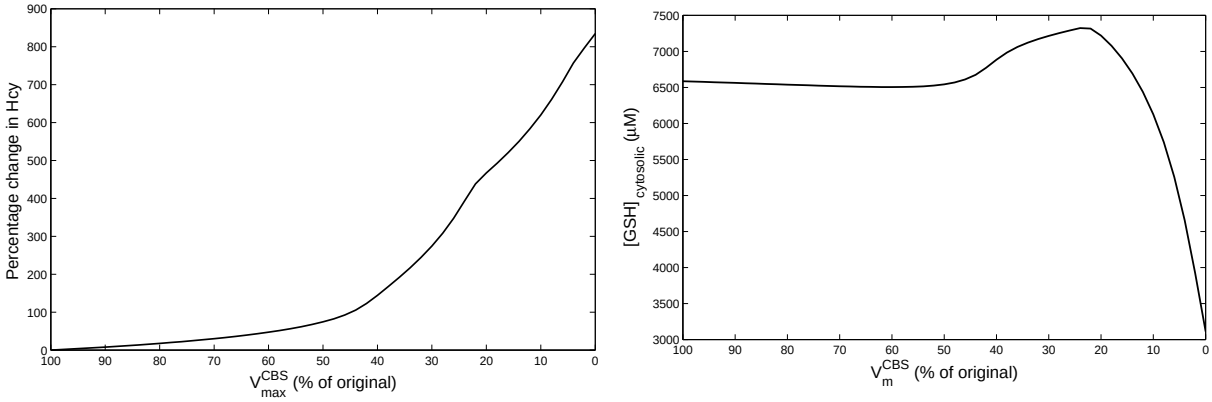

(a) (b)

Figure 7.2: **Inhibition of CBS leads to hyperhomocysteinemia and increased oxidative stress**. Steady state values of Hcy are seen to rise by over 800%, and cytosolic GSH values are seen plummeting, with increasing inhibition in CBS, a co-enzyme of vitamin B6. This shows us that inhibition of CBS is a necessary side-effect of vitamin B_{12} deficiency resulting in its symptoms: hyperhomocysteinemia and increased oxidative stress.

7.3 Hyperhomocysteinemia leads to increased GSH levels in the model

We artificially increase the Hcy levels in the Reed-Nijhout model by around 400% to simulate a hyperhomocysteinemic scenario. This leads to a phenomenal increase in the cytosolic GSH levels – by more than 200%.

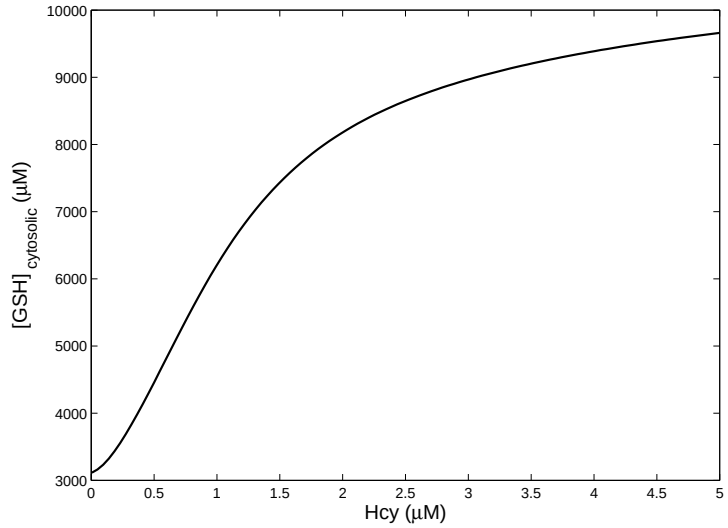

Figure 7.3: Hyperhomocysteinemia leads to increased cytosolic GSH levels. Cytosolic GSH levels are seen to rise by over 200% as Hcy levels are increased by a range of 400% in the Reed-Nijhout model. This figure leads one to assume that hyperhomocysteinemia has a positive effect on the oxidative stress in the cytosol.

While the plots observed in Fig. 7.3 are obvious from a naive look at the Reed-Nijhout model, this implies – rather intriguingly – that hyperhomocysteinemia, simulated by keeping all other parameters constant, plays a positive role in diabetic patients by increased activity against oxidative stress.

Chapter 8

Conclusions

Vitamin B_{12} activity in the cell is directly upstream of the GSH synthesis mechanism. Intrigued by the findings that GSH levels are uncorrelated to vitamin B_{12} levels (Fig. 2.1), we investigated the relationship between vitamin B_{12} and GSH in the Reed-Nijhout model. It turns out that the model shows Hcy, and metabolites downstream of it, maintain homeostatic behavior relative to changes in MS activity (Fig. 3.5).

We next investigated the reasons as to why Hcy exhibits homeostasis despite changes over several orders of magnitude in MS activity. We constructed a reduced model to approximate the methionine cycle, by carefully extracting the relevant sub-network from the Reed-Nijhout model. The reduced model is validated against the Reed-Nijhout model. Hcy is seen to be homeostatic to variation in MS activity even in the reduced model.

The reduced model suggested an even further simplification – a stylized model that reflects the topology of the methionine cycle. We derived the steady-state expressions for the metabolites in the stylized model to find that the homeostasis of Hcy is regulated by the value of k_{met}^{outmet}, the rate constant regulating the flux of Met our of the cytosol into blood (Fig 7.1). We tested this hypothesis in the reduced model and Reed-Nijhout model, and verified that a higher than normal value of k_{met}^{outmet} allows Hcy to vary considerably more with changes in MS activity.

Hyperhomocysteinemia is also associated with inhibition of CBS activity, a co-enzyme of vitamin B_6. Decreasing the CBS activity in the model, led to hyperhomocysteinemic conditions in the Reed-Nijhout model(Fig. 7.2).

By simulating hyperhomocysteinemia in the Reed-Nijhout model we confirm that hyperhomocysteinemia results in increased GSH levels (Fig. 7.3). Since our experimental data suggests a lack of correlation between vitamin B_{12} serum levels and GSH, we speculate that none of the vitamin B_{12} deficient individuals in our data were hyperhomocysteinemic, although we did not directly test for it. On the other hand, it should be noted that in case the vitamin B_{12} deficient individuals were also hyperhomocysteinemic, that could, in principle, arise through the CBS inhibition route; this mechanism would not allow for changes in Hcy to percolate further, to GSH.

Both experimental data and modeling suggest that GSH levels are unaffected by vitamin B_{12} levels. We conclude that although vitamin B_{12} deficiency strongly associated with vegetarianism, neither is likely to be the reason for the increased incidence of diabetes in the Indian subcontinent.

Appendices

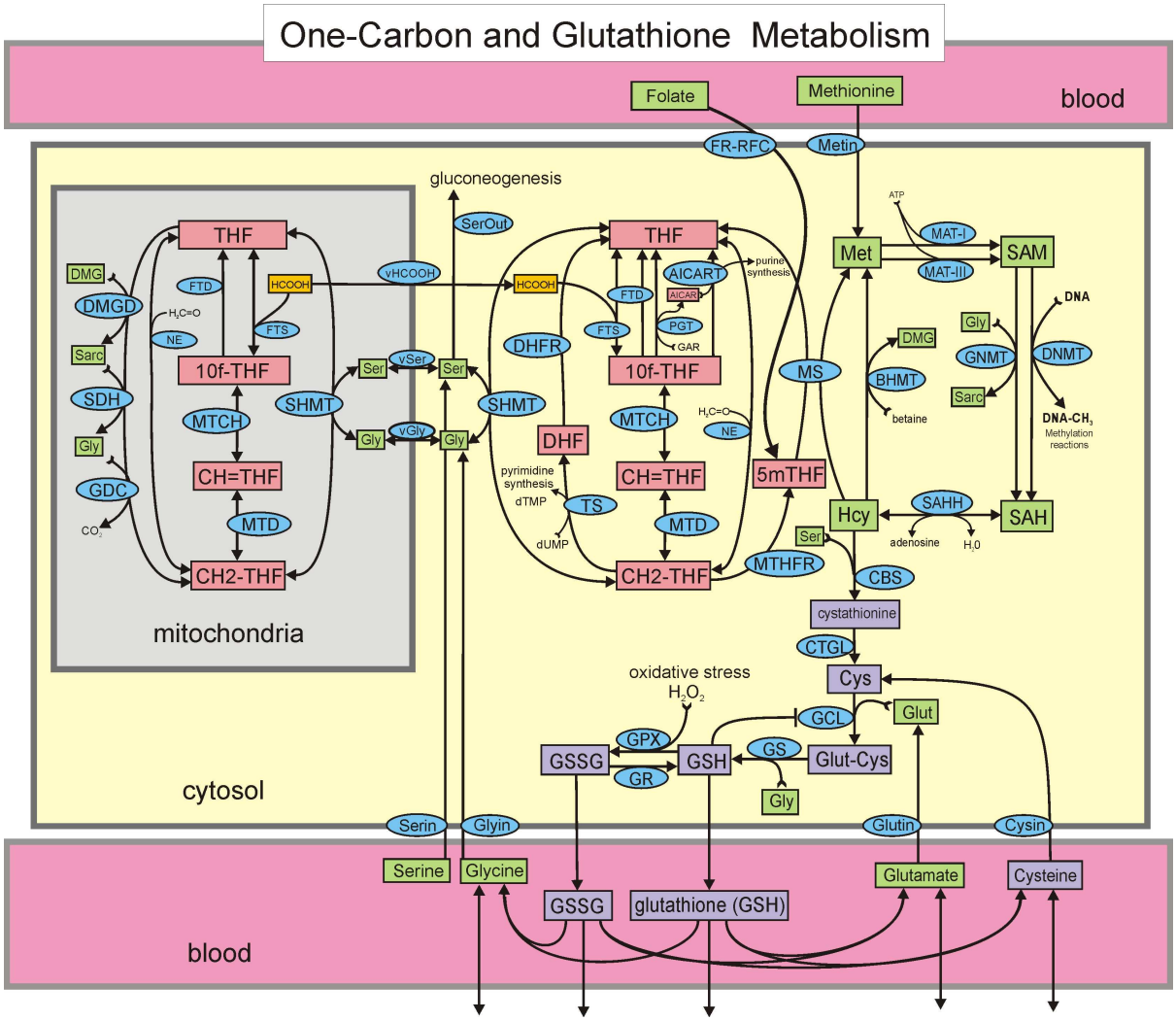

Figure 1: **One-carbon metabolism and glutathione synthesis.** Rectangular boxes indicate substrates that are variables in the model. Non-boxed substrates are either held constant in the model or are products of reactions. Each internal arrow indicates a biochemical reaction or transport reaction. The ellipses contain the acronyms of enzymes or transporters.

Bibliography

[1] Jhankar D Acharya, Amol J Pande, Suyog M Joshi, Chittaranjan S Yajnik, and Saroj S Ghaskadbi. Treatment of hyperglycemia in newly diagnosed diabetic patients is associated with a reduction in oxidative stress and improvement in β-cell function. *Diabetes/metabolism research and reviews*, 2014.

[2] M. C. Reed, R. L. Thomas, J. Pavisic, S. J. James, C. M. Ulrich, and H. F. Nijhout. A mathematical model of glutathione metabolism. *Theor Biol Med Model*, 5:8, 2008.

[3] A. C. Antony. Vegetarianism and vitamin B-12 (cobalamin) deficiency. *Am. J. Clin. Nutr.*, 78(1):3–6, Ju; 2003.

[4] S. P. Stabler and R. H. Allen. Vitamin B12 deficiency as a worldwide problem. *Annu. Rev. Nutr.*, 24:299–326, 2004.

[5] H. Refsum, C. S. Yajnik, M. Gadkari, J. Schneede, S. E. Vollset, L. Orning, A. B. Guttormsen, A. Joglekar, M. G. Sayyad, A. Ulvik, and P. M. Ueland. Hyperhomocysteinemia and elevated methylmalonic acid indicate a high prevalence of cobalamin deficiency in Asian Indians. *Am. J. Clin. Nutr.*, 74(2):233–241, Aug 2001.

[6] C. S. Yajnik, S. S. Deshpande, A. A. Jackson, H. Refsum, S. Rao, D. J. Fisher, D. S. Bhat, S. S. Naik, K. J. Coyaji, C. V. Joglekar, N. Joshi, H. G. Lubree, V. U. Deshpande, S. S. Rege, and C. H. Fall. Vitamin B12 and folate concentrations during pregnancy and insulin resistance in the offspring: the Pune Maternal Nutrition Study. *Diabetologia*, 51(1):29–38, Jan 2008.

[7] J. Selhub, M. S. Morris, and P. F. Jacques. In vitamin B12 deficiency, higher serum folate is associated with increased total homocysteine and methylmalonic acid concentrations. *Proc. Natl. Acad. Sci. U.S.A.*, 104(50):19995–20000, Dec 2007.

[8] M. C. Reed, H. F. Nijhout, M. L. Neuhouser, J. F. Gregory, B. Shane, S. J. James, A. Boynton, and C. M. Ulrich. A mathematical model gives insights into nutritional and genetic aspects of folate-mediated one-carbon metabolism. *J. Nutr.*, 136(10): 2653–2661, Oct 2006.

[9] M. C. Reed, H. F. Nijhout, R. Sparks, and C. M. Ulrich. A mathematical model of the methionine cycle. *J. Theor. Biol.*, 226(1):33–43, Jan 2004.

[10] H. F. Nijhout, M. C. Reed, P. Budu, and C. M. Ulrich. A mathematical model of the folate cycle: new insights into folate homeostasis. *J. Biol. Chem.*, 279(53): 55008–55016, Dec 2004.

[11] B. Deplancke and H. R. Gaskins. Redox control of the transsulfuration and glutathione biosynthesis pathways. *Curr Opin Clin Nutr Metab Care*, 5(1):85–92, Jan 2002.

[12] E. Albu, C. Filip, N. Zamosteanu, I. M. Jaba, I. S. Linic, and I. Sosa. Hyperhomocysteinemia is an indicator of oxidant stress. *Med. Hypotheses*, 78(4):554–555, Apr 2012.

[13] E. R. Hondorp and R. G. Matthews. Oxidative stress inactivates cobalamin-independent methionine synthase (MetE) in Escherichia coli. *PLoS Biol.*, 2(11): e336, Nov 2004.

[14] D. W. Jacobsen. Hyperhomocysteinemia and oxidative stress: time for a reality check? *Arterioscler. Thromb. Vasc. Biol.*, 20(5):1182–1184, May 2000.

[15] W. Herrmann, H. Schorr, R. Obeid, and J. Geisel. Vitamin B-12 status, particularly holotranscobalamin II and methylmalonic acid concentrations, and hyperhomocysteinemia in vegetarians. *Am. J. Clin. Nutr.*, 78(1):131–136, Jul 2003.

[16] R. V. Banerjee, V. Frasca, D. P. Ballou, and R. G. Matthews. Participation of cob(I) alamin in the reaction catalyzed by methionine synthase from Escherichia coli: a steady-state and rapid reaction kinetic analysis. *Biochemistry*, 29(50):11101–11109, Dec 1990.

[17] R. Banerjee, Z. Chen, and S. Gulati. Methionine synthase from pig liver. *Meth. Enzymol.*, 281:189–196, 1997.

[18] D. Watkins, M. Ru, H. Y. Hwang, C. D. Kim, A. Murray, N. S. Philip, W. Kim, H. Legakis, T. Wai, J. F. Hilton, B. Ge, C. Dore, A. Hosack, A. Wilson, R. A. Gravel, B. Shane, T. J. Hudson, and D. S. Rosenblatt. Hyperhomocysteinemia due to methionine synthase deficiency, cblG: structure of the MTR gene, genotype diversity, and recognition of a common mutation, P1173L. *Am. J. Hum. Genet.*, 71 (1):143–153, Jul 2002.

[19] Lukas Endler. European Bio-informatics Institute Bio-models Database. `http://www.ebi.ac.uk/compneur-srv/biomodels-main/publ-model.do?mid=BIOMD0000000268`, 2008. [Online].

[20] H. F. Nijhout, J. F. Gregory, C. Fitzpatrick, E. Cho, K. Y. Lamers, C. M. Ulrich, and M. C. Reed. A mathematical model gives insights into the effects of vitamin B-6 deficiency on 1-carbon and glutathione metabolism. *J. Nutr.*, 139(4):784–791, Apr 2009.